Accepted Manuscript

New analytic buckling solutions of rectangular thin plates with two free adjacent edges by the symplectic superposition method

Rui Li, Haiyang Wang, Xinran Zheng, Sijun Xiong, Zhaoyang Hu, Xiaoye Yan, Zhe Xiao, Houlin Xu, Peng Li

PII: S0997-7538(18)30325-5

DOI: https://doi.org/10.1016/j.euromechsol.2019.04.014

Reference: EJMSOL 3779

To appear in: *European Journal of Mechanics / A Solids*

Received Date: 2 May 2018

Revised Date: 4 April 2019

Accepted Date: 25 April 2019

Please cite this article as: Li, R., Wang, H., Zheng, X., Xiong, S., Hu, Z., Yan, X., Xiao, Z., Xu, H., Li, P., New analytic buckling solutions of rectangular thin plates with two free adjacent edges by the symplectic superposition method, *European Journal of Mechanics / A Solids* (2019), doi: https://doi.org/10.1016/j.euromechsol.2019.04.014.

New analytic buckling solutions of rectangular thin plates with two free adjacent edges by the symplectic superposition method

Rui Li[a,b,*], Haiyang Wang[a], Xinran Zheng[a], Sijun Xiong[a], Zhaoyang Hu[a], Xiaoye Yan[a], Zhe Xiao[a], Houlin Xu[a], Peng Li[c]

[a] *State Key Laboratory of Structural Analysis for Industrial Equipment, Department of Engineering Mechanics, and International Research Center for Computational Mechanics, Dalian University of Technology, Dalian 116024, China*

[b] *State Key Laboratory of Nonlinear Mechanics, Institute of Mechanics, Chinese Academy of Sciences, Beijing 100190, China*

[c] *Studienbereich Mechanik, Technische Universität Darmstadt, Darmstadt 64289, Germany*

[*] Corresponding author.
E-mail address: ruili@dlut.edu.cn (R. Li)

Abstract

This paper deals with a classic but very difficult type of problems, i.e., pursuing analytic buckling solutions of biaxially loaded rectangular thin plates with two free adjacent edges that are characterized by having both the free edges and a free corner. The primary challenge is to find the solutions satisfying both the governing high-order partial differential equations (PDEs) and non-Lévy-type boundary constraints. Here, an up-to-date symplectic superposition method is developed for the issues, which yields the analytic solutions by converting the problems to be solved into the superposition of two elaborated subproblems that are solved by the symplectic elasticity approach. The distinctive merit of the method is that a direct rigorous derivation helps to access the analytic solutions without any assumptions/prior knowledge of the solution forms, which is attributed to the implementation in the symplectic space-based Hamiltonian system rather than in the classic Euclidean space-based Lagrangian system. As the important outputs, comprehensive new analytic results are obtained, with 1200 critical buckling loads and 100 buckling mode shapes presented, which are all well validated by the refined finite element analysis. The rapid convergence and favorable accuracy of the present method make it competent as a benchmark one for similar problems.

Keywords: analytic solution; plate buckling; free edge; free corner; symplectic superposition method.

1. Introduction

Plates are widely used in various engineering structures, including bridge decks, ship superstructures, panels in aircrafts, column supported slabs in buildings, etc. There have been many investigations on the mechanical behaviors of the plates, among which the buckling under in-plane compressive loading represents a major mode of failure, and thus received much attention over the past decades. The key fundamental issue for plate buckling analysis involves seeking the critical buckling loads and associated buckling mode shapes, which are required to satisfy the governing high-order partial differential equations (PDEs) under prescribed boundary conditions, in an analytic way or by the numerical approaches. Therefore, the solution methods are of much importance in handling the buckling problems of plates.

Various effective numerical methods have been developed to conduct the buckling analysis of plates. For a brief overview of the recent progress in the field, some typical methods are introduced in this paragraph. Ravari et al. (2013, 2014) used the finite difference method to study the buckling behavior of both rectangular and circular annular nanoplates; the method was proved to be powerful for determination of the buckling loads as well as buckling modes with little computational effort. Moradi and Taheri (1999) investigated the delamination buckling response of a composite panel containing through-the-width delamination by the implementation of the differential quadrature (DQ) technique, which exhibited high efficiency in treating similar problems. Civalek et al. (2010, 2008) adopted the discrete singular convolution method for buckling analysis of plate structures, which demonstrated the suitability of the method for the problems considered due to its simplicity. Li et al. (2016a) employed a transfer function method to study the buckling response of rectangular plates resting on tensionless foundations, revealing that the boundary conditions at the loaded edges (end conditions) significantly affect the contact buckling performance. Lopatin and Morozov (2014) carried out an approximate buckling analysis of a rectangular orthotropic plate with two opposite edges clamped and another two edges free using the generalized Galerkin method, which could facilitate quick, reliable and accurate calculations of the critical buckling loads. Bui et al. (2011) proposed a meshfree moving Kriging interpolation method incorporating the shear-locking elimination technique for buckling analysis of thick plates, which was proved to be robust, effective and highly accurate. Natarajan et al. (2014) studied the effect of local defects on the buckling behavior of functionally graded material plates subjected to mechanical and thermal load by the partition of unity method, providing a useful guideline for the design of plates with cracks and cutouts. Lal and Ahlawat (2015) took the differential transform method to successfully solve the differential equation governing the dynamic buckling of simply supported and clamped functionally graded circular plates subjected to uniform in-plane force. Meziane et al. (2014) presented an efficient and simple refined theory for buckling and free vibration of exponentially graded sandwich plates under various boundary conditions, where a method with approximate admissible functions was adopted for solution. Similar solution methods were also adopted for functionally graded sandwich plates (Abdelaziz et al., 2017) and shear-deformable composite beams (Kaci et al., 2018). Except for the newly developed methods, some classic methods, with proper modifications or new applications, are still prevalent for solving the buckling problems of various plates, e.g., the Ritz energy method (Mijuskovic et al., 2015; Mirzaei and Kiani, 2016) and finite element method (FEM) (Asemi et al., 2015; Jeyaraj, 2013; Komur and Sonmez, 2015).

It is noted that the advanced numerical methods are often qualified for the buckling solutions of plates with acceptable errors such that they have been widely adopted as effective tools for the analyses and designs, especially for the plates with complex loading and boundary conditions. Nevertheless, developing novel analytic approaches as well as pursuing new analytic solutions is still a crucial issue, which is essential for the development of the plate theory. It is well acknowledged that the analytic solutions are valuable for providing the benchmark results for validation of various numerical/approximate methods, and are very useful for rapid parametric analysis and optimization. Despite this, analytic buckling solutions of plates have been far from complete due to the difficulty in exploring the solutions that satisfy the high-order PDEs under prescribed boundary constraints. In recent years, very few novel analytic methods/solutions have been found for plate buckling problems. For example, an analytic method for decoupling the coupled stability equations was introduced for moderately thick functionally graded rectangular plates with two opposite edges simply supported by Mohammadi et al. (2010), and for moderately thick functionally graded sector and annular sector plates with simply supported edges by Naderi and Saidi (2011a, b). An optimized hyperbolic unified formulation was presented by Mantari and Monge (2016) for analytic buckling solutions of simply supported functionally graded sandwich plates. The classic variables separation method was applied by Moslemi et al. (2017) to solve the buckling problems of thick rectangular transversely isotropic simply supported plates. While finding that some new analytic approaches have been derived, it is noted that the main deficiency in the field is that the analytic solutions were mostly restricted to the Lévy-type plates (i.e., those with at least two opposite edges simply supported), but there have been rare reports on the non-Lévy-type plates that are more commonly encountered in engineering practice. This situation motivates the present exploration of new analytic solutions that have not been reported.

We recently proposed a novel analytic symplectic superposition method with applications to some plate problems such as bending (Li et al., 2015a; Li et al., 2017; Li et al., 2015b), vibration (Li et al., 2016b; Li et al., 2018) and buckling (Wang et al., 2016). The method skillfully combines the superposition method and symplectic elasticity approach that was pioneered by Yao et al. (2009) and well extended by Lim et al. (Lim, 2010; Lim et al., 2009; Lim and Xu, 2010) and Li et al. (2015a, 2016b, 2015b, 2018) for plate problems. The solution procedure involves converting the problem to be solved into the superposition of several elaborated subproblems that can be solved by the symplectic elasticity approach. The method is realized in the symplectic space-based Hamiltonian system, which is quite different from any other analytic methods that are implemented in the Euclidean space and Lagrangian system. The primary advantage of the method is the potential of access to more analytic solutions because it is inherently rigorous without assumptions on the solution forms, which cannot be achieved by the classic semi-inverse methods. Till now, the only buckling problem that has been solved by the symplectic superposition method is for a uniaxially compressed rectangular thin plate with combinations of simply supported and clamped edges, but there has been no report of its extension to non-Lévy-type plates with free edges, which are more difficult issues and have not been well figured out (Wang et al., 2016).

The objective of this paper is to further develop the symplectic superposition method for accurate buckling analysis of biaxially loaded rectangular thin plates with two free adjacent edges. This class of problems has the feature of having both the free edges and a free corner in a plate, which increases the solution difficulty. Three types of boundary conditions for the plates are studied, i.e., those with two adjacent edges free and the other two edges **(i)** clamped (CCFF), **(ii)** simply supported (SSFF), or **(iii)** clamped-simply supported (CSFF). Here, anticlockwise denotation of the boundary conditions is adopted for a plate, starting from the bottom edge (Fig. 1a), with "F"=free, "C"=clamped, and "S"=simply supported. Comprehensive analytic results are obtained and shown in ten tables and ten figures, corresponding to 1200 numerical results for critical buckling loads and 100 buckling mode shapes, respectively. Very rapid convergence is observed for all of the present solutions by the convergence study, as reflected in another ten tables. Very good agreement with the FEM validates the present solutions, which can be regarded as the benchmarks for comparison with the future numerical/approximate approaches.

2. Governing equation and fundamental symplectic analytic solutions in the Hamiltonian system

2.1. Governing equation of a buckled plate in the Hamiltonian system

Applying the Hellinger-Reissner variational principle in combination with the Lagrangian multiplier method, the governing equations of a buckled thin plate occupying the domain Ω in the rectangular coordinate system *oxy* can be described by the following Hamiltonian system-based variational principle (Wang et al., 2016):

$$\begin{aligned}\delta\Pi_H = \delta\iint_{\Omega}\Bigg\{&\frac{D}{2}\left(\frac{\partial^2 w}{\partial x^2}\right)^2+\frac{D}{2}\left(\frac{\partial\theta}{\partial y}\right)^2+D\nu\frac{\partial^2 w}{\partial x^2}\frac{\partial\theta}{\partial y}+D(1-\nu)\left(\frac{\partial\theta}{\partial x}\right)^2\\&-\frac{D}{2(1-\nu^2)}\left(\frac{M_y}{D}+\frac{\partial\theta}{\partial y}+\nu\frac{\partial^2 w}{\partial x^2}\right)^2+T\left(\theta-\frac{\partial w}{\partial y}\right)\\&+\frac{1}{2}\left[N_x\left(\frac{\partial w}{\partial x}\right)^2+N_y\theta^2+2N_{xy}\left(\frac{\partial w}{\partial x}\right)\theta\right]\Bigg\}dxdy\\&=0\end{aligned} \tag{1}$$

Here, Π_H is the Hamiltonian functional; w is the out-of-plane deflection of the plate; D is the flexural stiffness; ν is the Poisson's ratio; T is the Lagrangian multiplier; θ is an introduced quantity. The internal forces per unit distance in the plate include the shearing forces Q_x and Q_y, bending moments M_x and M_y, twisting moment M_{xy}, shearing membrane force N_{xy}, and normal membrane forces N_x and N_y. The constant normal membrane forces and zero shearing membrane force are assumed for convenience. According to Eq. (1), we obtain

$$\frac{\partial \mathbf{Z}}{\partial y} = \mathbf{HZ} \tag{2}$$

where $\mathbf{Z} = \left[w, \theta, T, M_y\right]^{\mathrm{T}}$, $\mathbf{H} = \begin{bmatrix} \mathbf{F} & \mathbf{G} \\ \mathbf{Q} & -\mathbf{F}^{\mathrm{T}} \end{bmatrix}$, $\mathbf{F} = \begin{bmatrix} 0 & 1 \\ -\nu \partial^2/\partial x^2 & 0 \end{bmatrix}$, $\mathbf{G} = \begin{bmatrix} 0 & 0 \\ 0 & -1/D \end{bmatrix}$, and $\mathbf{Q} = \begin{bmatrix} -D\left(1-\nu^2\right)\partial^4/\partial x^4 + N_x \partial^2/\partial x^2 & 0 \\ 0 & 2D(1-\nu)\partial^2/\partial x^2 - N_y \end{bmatrix}$. It is obtained from Eq. (2) that $\theta = \partial w/\partial y$ and $T = -V_y$, with $V_y = Q_y + \frac{\partial M_{xy}}{\partial x} + N_y \frac{\partial w}{\partial y}$ being the equivalent shearing force. $\mathbf{H}$ is a Hamiltonian operator matrix satisfying $\mathbf{H}^{\mathrm{T}} = \mathbf{JHJ}$, in which $\mathbf{J} = \begin{bmatrix} 0 & \mathbf{I}_2 \\ -\mathbf{I}_2 & 0 \end{bmatrix}$ is the symplectic matrix with $\mathbf{I}_2$ being the 2×2 unit matrix (Yao et al., 2009). Therefore, Eq. (2) serves as the governing dual equation of the buckled plate in the Hamiltonian system, with the generalized displacements (w and θ) and generalized forces (T and M_y) being the dual variables.

2.2. Fundamental symplectic analytic solutions for the subproblems

Buckling of a CCFF rectangular thin plate with length *a* and width *b* (Fig. 1a) is focused on, which is converted into the superposition of two elaborated subproblems, as shown in Figs. 1b and 1c. The biaxial uniform in-plane loads with intensity κP and γP are applied in the *x*- and *y*- directions, respectively, where κ and γ are the loading coefficients that govern the load magnitudes. Uniaxial loading is realized when either κ or γ becomes zero. In the first subproblem, the edge along $x = 0$ is slidingly clamped, and that along $x = a$ is simply supported. The slope represented by $\Sigma_{n=1,3,5,\cdots}^{\infty} E_n \cos\left(\alpha_n x\right)$ and bending moment represented by $\Sigma_{n=1,3,5,\cdots}^{\infty} F_n \cos\left(\alpha_n x\right)$ are applied along the slidingly clamped edge at $y = 0$ and simply supported edge at $y = b$, respectively. Another subproblem is on the plate with $y = 0$ slidingly clamped and $y = b$ simply supported. The slope represented by $\Sigma_{n=1,3,5,\cdots}^{\infty} G_n \cos\left(\beta_n y\right)$ and bending moment represented by $\Sigma_{n=1,3,5,\cdots}^{\infty} H_n \cos\left(\beta_n y\right)$ are distributed along the slidingly clamped edge at $x = 0$ and simply supported edge at $x = a$, respectively. Here, $\alpha_n = n\pi/(2a)$, $\beta_n = n\pi/(2b)$, E_n, F_n, G_n and H_n are the coefficients of the half-cosine series expansion.

Substituting $N_x = -\kappa P$ and $N_y = -\gamma P$ into Eq. (2), we have the governing equation of the first subproblem (Fig. 1b). Exchanging x and y, a and b, and κ and γ, we have the governing equation of the second subproblem (Fig. 1c). In the symplectic space, the separation of variables holds for solving Eq. (2), i.e., $\mathbf{Z} = \mathbf{X}(x)Y(y)$, with $\mathbf{X}(x) = \left[w(x), \theta(x), T(x), M_y(x)\right]^{\mathrm{T}}$ as a unary vector of x and $Y(y)$ a unary function of y. Therefore, $\mathrm{d}Y(y)/\mathrm{d}y = \mu Y(y)$ and $\mathbf{HX}(x) = \mu\mathbf{X}(x)$ are deduced from Eq. (2), where μ and $\mathbf{X}(x)$ are respectively the eigenvalue and eigenvector of the Hamiltonian matrix $\mathbf{H}$. Applying the boundary conditions $\partial w(x)/\partial x\big|_{x=0} = V_x(x)\big|_{x=0} = 0$ and $w(x)\big|_{x=a} = M_x(x)\big|_{x=a} = 0$, the eigenvalues and eigenvectors for the first subproblem are

$$\begin{aligned} \mu_{1n} &= \sqrt{\alpha_n^2 - \gamma R/2 + \sqrt{R\left[\kappa\alpha_n^2 + \gamma\left(\gamma R/4 - \alpha_n^2\right)\right]}} \\ \mu_{2n} &= -\mu_{1n} \\ \mu_{3n} &= \sqrt{\alpha_n^2 - \gamma R/2 - \sqrt{R\left[\kappa\alpha_n^2 + \gamma\left(\gamma R/4 - \alpha_n^2\right)\right]}} \\ \mu_{4n} &= -\mu_{3n} \end{aligned} \tag{3}$$

and

$$\mathbf{X}_{in} = \left\{1, \mu_{in}, D\left(\nu\alpha_n^2 - \mu_{in}^2\right), D\mu_{in}\left[\mu_{in}^2 + (\nu - 2)\alpha_n^2 + \gamma R\right]\right\}^{\mathrm{T}} \cos(\alpha_n x) \tag{4}$$

for n=1, 3, 5, … (i=1, 2, 3 and 4), where $R = P/D$.

Based on the eigenvectors for the first subproblem, the state vector $\mathbf{Z}$ is expanded according to the symplectic orthogonality and conjugacy (Yao et al., 2009), yielding

$$\mathbf{Z} = \sum_{n=1,3,5,\cdots}^{\infty} \sum_{i=1}^{4} C_{in} e^{\mu_{in} y} \mathbf{X}_{in} \tag{5}$$

The mode shape function, denoted by $w_1(x, y)$, is thus obtained by

$$w_1(x, y) = \sum_{n=1,3,5,\cdots}^{\infty} \sum_{i=1}^{4} C_{in} e^{\mu_{in} y} \cos(\alpha_n x) \tag{6}$$

where the constants C_{in} (n=1, 3, 5, …; i=1, 2, 3 and 4) are determined by substituting the boundary conditions at y=0 and y=b,

$$\begin{aligned} &T\big|_{y=0} = 0 \\ &\theta\big|_{y=0} = \sum_{n=1,3,5,\ldots}^{\infty} E_n \cos(\alpha_n x) \\ &w_1\big|_{y=b} = 0 \\ &M_y\big|_{y=b} = \sum_{n=1,3,5,\ldots}^{\infty} F_n \cos(\alpha_n x) \end{aligned} \tag{7}$$

into Eq. (5). The out-of-plane deflection solution is thus obtained as

$$\begin{aligned} w_1(x,y) = &\sum_{n=1,3,5,\cdots}^{\infty} \frac{\cos(\alpha_n x)}{D\mu_{1n}\mu_{3n}\left(\mu_{1n}^2 - \mu_{3n}^2\right)} \\ &\times\Big\{D\big\{\varepsilon_n\left[\mathrm{sh}(\mu_{3n}y) - \mathrm{th}(\mu_{3n}b)\mathrm{ch}(\mu_{3n}y)\right] - \zeta_n\left[\mathrm{sh}(\mu_{1n}y) - \mathrm{th}(\mu_{1n}b)\mathrm{ch}(\mu_{1n}y)\right]\big\}E_n \\ &+\mu_{1n}\mu_{3n}\left[\mathrm{sech}(\mu_{3n}b)\mathrm{ch}(\mu_{3n}y) - \mathrm{sech}(\mu_{1n}b)\mathrm{ch}(\mu_{1n}y)\right]F_n\Big\} \end{aligned} \tag{8}$$

where $\varepsilon_n = \mu_{1n}\left[R\gamma + \mu_{1n}^2 - (2-\nu)\alpha_n^2\right]$ and $\zeta_n = \mu_{3n}\left[R\gamma + \mu_{3n}^2 - (2-\nu)\alpha_n^2\right]$. Using the coordinates exchange (Exchanging x and y, a and b, κ and γ, and replacing E_n with G_n, and F_n with H_n), the solution of the second subproblem (Fig. 1c), denoted by $w_2(x,y)$, can be simply obtained.

3. Analytic buckling solutions of the plates with two free adjacent edges

For a CCFF plate, zero bending moment must be satisfied at $x=0$ and $y=0$, and zero slope must be satisfied at $x=a$ and $y=b$, i.e.,

$$\begin{aligned} &\sum_{i=1}^{2}\left(\frac{\partial^2 w_i}{\partial x^2} + \nu\frac{\partial^2 w_i}{\partial y^2}\right)\Bigg|_{x=0} = 0 \\ &\sum_{i=1}^{2}\left(\frac{\partial^2 w_i}{\partial y^2} + \nu\frac{\partial^2 w_i}{\partial x^2}\right)\Bigg|_{y=0} = 0 \\ &\sum_{i=1}^{2}\frac{\partial w_i}{\partial x}\Bigg|_{x=a} = 0 \\ &\sum_{i=1}^{2}\frac{\partial w_i}{\partial y}\Bigg|_{y=b} = 0 \end{aligned} \tag{9}$$

Substituting Eq. (8) (for $w_1(x,y)$) and its variant (for $w_2(x,y)$) into Eq. (9), and expanding the polynomials that arise as the half-cosine series, followed by comparison of coefficients, we have the following equivalent conditions of Eq. (9). For $x=0$, we have

$$D\left[\xi_i \operatorname{th}\left(a\tilde{\mu}_{1i}\right)\left(\tilde{\mu}_{1i}^2-\nu\beta_i^2\right)-\eta_i \operatorname{th}\left(a\tilde{\mu}_{3i}\right)\left(\tilde{\mu}_{3i}^2-\nu\beta_i^2\right)\right]G_i$$
$$-\tilde{\mu}_{1i}\tilde{\mu}_{3i}\left[\operatorname{sech}\left(a\tilde{\mu}_{1i}\right)\left(\tilde{\mu}_{1i}^2-\nu\beta_i^2\right)-\operatorname{sech}\left(a\tilde{\mu}_{3i}\right)\left(\tilde{\mu}_{3i}^2-\nu\beta_i^2\right)\right]H_i$$
$$-\sum_{n=1,3,5,\cdots}^{\infty}\frac{\tilde{\mu}_{1i}\tilde{\mu}_{3i}\left(\tilde{\mu}_{1i}^2-\tilde{\mu}_{3i}^2\right)}{\left(\pi^2 i^2+4b^2\mu_{1n}^2\right)\left(\pi^2 i^2+4b^2\mu_{3n}^2\right)} \tag{10}$$
$$\times\left\{\frac{8bD\left[\zeta_n\mu_{1n}\left(\alpha_n^2-\nu\mu_{1n}^2\right)\left(\pi^2 i^2+4b^2\mu_{3n}^2\right)-\varepsilon_n\mu_{3n}\left(\alpha_n^2-\nu\mu_{3n}^2\right)\left(\pi^2 i^2+4b^2\mu_{1n}^2\right)\right]}{\mu_{1n}\mu_{3n}\left(\mu_{1n}^2-\mu_{3n}^2\right)}E_n\right.$$
$$\left.+4\pi i\left(\nu\pi^2 i^2+4b^2\alpha_n^2\right)\sin\left(\frac{\pi i}{2}\right)F_n\right\}=0$$

for $i=1,3,5,\cdots$; for $y=0$, we have

$$D\left[\zeta_i \operatorname{th}\left(b\mu_{1i}\right)\left(\mu_{1i}^2-\nu\alpha_i^2\right)-\varepsilon_i \operatorname{th}\left(b\mu_{3i}\right)\left(\mu_{3i}^2-\nu\alpha_i^2\right)\right]E_i$$
$$-\mu_{1i}\mu_{3i}\left[\operatorname{sech}\left(b\mu_{1i}\right)\left(\mu_{1i}^2-\nu\alpha_i^2\right)-\operatorname{sech}\left(b\mu_{3i}\right)\left(\mu_{3i}^2-\nu\alpha_i^2\right)\right]F_i$$
$$-\sum_{n=1,3,5,\cdots}^{\infty}\frac{\mu_{1i}\mu_{3i}\left(\mu_{1i}^2-\mu_{3i}^2\right)}{\left(\pi^2 i^2+4a^2\tilde{\mu}_{1n}^2\right)\left(\pi^2 i^2+4a^2\tilde{\mu}_{3n}^2\right)}$$
$$\times\left\{\frac{8aD\left[\xi_n\tilde{\mu}_{1n}\left(\beta_n^2-\nu\tilde{\mu}_{1n}^2\right)\left(\pi^2 i^2+4a^2\tilde{\mu}_{3n}^2\right)-\eta_n\tilde{\mu}_{3n}\left(\beta_n^2-\nu\tilde{\mu}_{3n}^2\right)\left(\pi^2 i^2+4a^2\tilde{\mu}_{1n}^2\right)\right]}{\tilde{\mu}_{1n}\tilde{\mu}_{3n}\left(\tilde{\mu}_{1n}^2-\tilde{\mu}_{3n}^2\right)}G_n\right.$$
$$\left.+4\pi i\left(\nu\pi^2 i^2+4a^2\beta_n^2\right)\sin\left(\frac{\pi i}{2}\right)H_n\right\}=0 \tag{11}$$

for $i=1,3,5,\cdots$; for $x=a$, we have

$$D\left[\xi_i\tilde{\mu}_{1i}\operatorname{sech}\left(a\tilde{\mu}_{1i}\right)-\eta_i\tilde{\mu}_{3i}\operatorname{sech}\left(a\tilde{\mu}_{3i}\right)\right]G_i$$
$$+\tilde{\mu}_{1i}\tilde{\mu}_{3i}\left[\tilde{\mu}_{1i}\operatorname{th}\left(a\tilde{\mu}_{1i}\right)-\tilde{\mu}_{3i}\operatorname{th}\left(a\tilde{\mu}_{3i}\right)\right]H_i$$
$$-\sum_{n=1,3,5,\cdots}^{\infty}\frac{\tilde{\mu}_{1i}\tilde{\mu}_{3i}\left(\tilde{\mu}_{1i}^2-\tilde{\mu}_{3i}^2\right)}{\left(\pi^2 i^2+4b^2\mu_{1n}^2\right)\left(\pi^2 i^2+4b^2\mu_{3n}^2\right)} \tag{12}$$
$$\times\left\{\frac{8Db\alpha_n\sin\left(a\alpha_n\right)\left[\pi^2 i^2\left(\varepsilon_n\mu_{3n}-\zeta_n\mu_{1n}\right)+4b^2\mu_{1n}\mu_{3n}\left(\varepsilon_n\mu_{1n}-\zeta_n\mu_{3n}\right)\right]}{\mu_{1n}\mu_{3n}\left(\mu_{1n}^2-\mu_{3n}^2\right)}E_n\right.$$
$$\left.-16\pi i\alpha_n b^2\sin\left(a\alpha_n\right)\sin\left(\frac{\pi i}{2}\right)F_n\right\}=0$$

for $i=1,3,5,\cdots$; and for $y=b$, we have

$$
\begin{aligned}
& D\left[\zeta_i \mu_{1i} \operatorname{sech}\left(b\mu_{1i}\right) - \varepsilon_i \mu_{3i} \operatorname{sech}\left(b\mu_{3i}\right)\right] E_i \\
& + \mu_{1i}\mu_{3i}\left[\mu_{1i} \operatorname{th}\left(b\mu_{1i}\right) - \mu_{3i} \operatorname{th}\left(b\mu_{3i}\right)\right] F_i \\
& - \sum_{n=1,3,5,\cdots}^{\infty} \frac{\mu_{1i}\mu_{3i}\left(\mu_{1i}^2 - \mu_{3i}^2\right)}{\left(\pi^2 i^2 + 4a^2 \tilde{\mu}_{1n}^2\right)\left(\pi^2 i^2 + 4a^2 \tilde{\mu}_{3n}^2\right)} \\
& \times \left\{ \frac{8Da\beta_n \sin\left(b\beta_n\right)\left[\pi^2 i^2 \left(\eta_n \tilde{\mu}_{3n} - \xi_n \tilde{\mu}_{1n}\right) + 4a^2 \tilde{\mu}_{1n}\tilde{\mu}_{3n}\left(\eta_n \tilde{\mu}_{1n} - \xi_n \tilde{\mu}_{3n}\right)\right]}{\tilde{\mu}_{1n}\tilde{\mu}_{3n}\left(\tilde{\mu}_{1n}^2 - \tilde{\mu}_{3n}^2\right)} G_n \right. \\
& \left. - 16\pi i \beta_n a^2 \sin\left(b\beta_n\right) \sin\left(\frac{\pi i}{2}\right) H_n \right\} = 0
\end{aligned} \tag{13}
$$

for $i = 1, 3, 5, \cdots$. Here,

$\mu_{1i} = \sqrt{\alpha_i^2 - \gamma R/2 + \sqrt{R\left[\kappa\alpha_i^2 + \gamma\left(\gamma R/4 - \alpha_i^2\right)\right]}}$, $\mu_{3i} = \sqrt{\alpha_i^2 - \gamma R/2 - \sqrt{R\left[\kappa\alpha_i^2 + \gamma\left(\gamma R/4 - \alpha_i^2\right)\right]}}$,

$\tilde{\mu}_{1i} = \sqrt{\beta_i^2 - \kappa R/2 + \sqrt{R\left[\gamma\beta_i^2 + \kappa\left(\kappa R/4 - \beta_i^2\right)\right]}}$, $\tilde{\mu}_{3i} = \sqrt{\beta_i^2 - \kappa R/2 - \sqrt{R\left[\gamma\beta_i^2 + \kappa\left(\kappa R/4 - \beta_i^2\right)\right]}}$,

$\tilde{\mu}_{1n} = \sqrt{\beta_n^2 - \kappa R/2 + \sqrt{R\left[\gamma\beta_n^2 + \kappa\left(\kappa R/4 - \beta_n^2\right)\right]}}$, $\tilde{\mu}_{3n} = \sqrt{\beta_n^2 - \kappa R/2 - \sqrt{R\left[\gamma\beta_n^2 + \kappa\left(\kappa R/4 - \beta_n^2\right)\right]}}$,

$\varepsilon_i = \mu_{1i}\left[R\gamma + \mu_{1i}^2 - (2-\nu)\alpha_i^2\right]$, $\zeta_i = \mu_{3i}\left[R\gamma + \mu_{3i}^2 - (2-\nu)\alpha_i^2\right]$, $\eta_i = \tilde{\mu}_{1i}\left[R\kappa + \tilde{\mu}_{1i}^2 - (2-\nu)\beta_i^2\right]$,

$\xi_i = \tilde{\mu}_{3i}\left[R\kappa + \tilde{\mu}_{3i}^2 - (2-\nu)\beta_i^2\right]$, $\eta_n = \tilde{\mu}_{1n}\left[R\kappa + \tilde{\mu}_{1n}^2 - (2-\nu)\beta_n^2\right]$, $\xi_n = \tilde{\mu}_{3n}\left[R\kappa + \tilde{\mu}_{3n}^2 - (2-\nu)\beta_n^2\right]$,

$\alpha_i = i\pi/(2a)$, and $\beta_i = i\pi/(2b)$.

It is obvious that the constants in Eqs. (10)-(13) cannot be all zero, otherwise there is no buckling for the plate. The existence of non-zero solutions requires that the determinant of the coefficient matrix given by the four sets of simultaneous homogeneous algebraic equations with respect to E_n, F_n, G_n and H_n ($n = 1, 3, 5, \cdots$) be zero, from which we obtain the critical buckling load solutions. Substitution of a set of non-zero constant solutions into Eq. (8) (for $w_1(x, y)$) and its variant (for $w_2(x, y)$), followed by their summation, the mode shape solutions are obtained. It is appreciated that the solutions can be obtained as accurate as desired by increasing the series terms in calculation.

The other cases of the plates with two free adjacent edges, i.e., CSFF and SSFF plates, can be easily deduced from the solutions of CCFF plates. By equating H_n ($n = 1, 3, 5, ...$) to zero and eliminating Eq. (12), solving the remaining three sets of equations yields the solutions of CSFF plates. By equating both F_n and H_n to zero and eliminating both Eqs. (12) and (13), solving the remaining two sets of equations yields the solutions of SSFF plates.

4. Comprehensive numerical and graphical results

Comprehensive numerical results for critical buckling loads and graphical results for buckling mode shapes of CCFF, CSFF and SSFF plates with $\nu = 0.25$ under both uniaxial or biaxial in-plane compressive loads are presented in this section to demonstrate the validity of the symplectic superposition method and accuracy of the analytic solutions obtained. The non-dimensional critical buckling loads, $P_{cr}b^2/(\pi^2 D)$, are compared with those by FEM via the commercial software ABAQUS (2013), where the thickness-to-width ratio of the plates is uniformly set to be 10^{-3}, and the thin shell element with the uniform size of $1/400$ of the minimum in-plane dimension are taken to give the numerical solutions as reliable as possible.

We first consider the plates with 12 different aspect ratios subjected to uniaxial loads. For CCFF and SSFF plates, the loads can be applied in either *x*- ($\kappa = 1$, $\gamma = 0$) or *y*- ($\kappa = 0$, $\gamma = 1$) direction due to symmetry, but the two loading cases should be differentiated for CSFF plates. Accordingly, four examples are examined, with the first ten non-dimensional critical buckling loads tabulated in Tables 1-4, respectively. The corresponding first ten buckling mode shapes of square plates are illustrated in Figs. 2-5, respectively. We then focus on the plates with the same aspect ratios as above but subjected to biaxial loads. Both $\kappa = 1$, $\gamma = 1$ and $\kappa = 1$, $\gamma = 5$ are investigated for each type of plates. Tables 5 and 6, 7 and 8, 9 and 10 give the first ten non-dimensional critical buckling loads for CCFF, SSFF and CSFF plates, respectively. Figures 6-11 plot the corresponding first ten buckling mode shapes of square plates. The convergence study is performed for all the present cases. Corresponding to Tables 1-10, the plates with *a*/*b*=0.4 and 4.5 are examined for each case, as shown in Tables 11-20. It is found that the present solutions converge rapidly, with only tens of series terms yielding sufficient accuracy, as reflected by the bold convergent results. For convenience, 80 series terms are adopted throughout this study to ensure the five significant figures accuracy. It is noted that all the current solutions, including both the critical buckling loads and mode shapes, agree very well with FEM; thus, the validity and accuracy of the new analytic method and solutions are well confirmed.

5. Conclusions

The new analytic buckling solutions of rectangular thin plates with two free adjacent edges are obtained by the symplectic superposition method. Since the present solution procedure avoids any predeterminations of the solution forms, it offers a novel approach to tackling the buckling problems of plates without two opposite edges simply supported, which can rationally yield more analytic solutions that cannot be achieved by conventional analytic methods. The issues that are settled in this study represent one of the most difficult classes since both the free edges and free corner have been involved. A large number of numerical and graphical results for CCFF, SSFF and CSFF plates provide useful benchmarks for future studies. The follow-up work based on the symplectic superposition method may involve bending, vibration, and buckling of the plates with inhomogeneous materials such as the functionally graded materials (Mahi and Tounsi, 2015; Bousahla et al., 2016; Bellifa et al., 2017). Some variants of the thin plate structures such as thick plates, sandwich plates, and cross-ply laminated plates (Bouderba et al., 2016; El-Haina et al., 2017; Menasria et al., 2017; Chikh et al., 2017) may also be investigated under the same solution framework.

Acknowledgements

The authors gratefully acknowledge the support from the Young Elite Scientists Sponsorship Program by CAST (grant 2015QNRC001), National Basic Research Program of China (grant 2014CB049000), Opening Fund of State Key Laboratory of Nonlinear Mechanics, and Fundamental Research Funds for the Central Universities (grant DUT18GF101).

References

ABAQUS, 2013. Analysis User's Guide V6.13. Dassault Systèmes, Pawtucket, RI.

Abdelaziz, H.H., Meziane, M.A.A., Bousahla, A.A., Tounsi, A., Mahmoud, S.R., Alwabli, A.S., 2017. An efficient hyperbolic shear deformation theory for bending, buckling and free vibration of FGM sandwich plates with various boundary conditions. Steel and Composite Structures 25, 693-704.

Asemi, K., Salehi, M., Akhlaghi, M., 2015. Three dimensional graded finite element elasticity shear buckling analysis of FGM annular sector plates. Aerospace Science and Technology 43, 1-13.

Bellifa, H., Bakora, A., Tounsi, A., Bousahla, A.A., Mahmoud, S.R., 2017. An efficient and simple four variable refined plate theory for buckling analysis of functionally graded plates. Steel and Composite Structures 25, 257-270.

Bousahla, A.A., Benyoucef, S., Tounsi, A., Mahmoud, S.R., 2016. On thermal stability of plates with functionally graded coefficient of thermal expansion. Structural Engineering and Mechanics 60, 313-335.

Bouderba, B., Houari, M.S.A., Tounsi, A., Mahmoud, S.R., 2016. Thermal stability of functionally graded sandwich plates using a simple shear deformation theory. Structural Engineering and Mechanics 58, 397-422.

Bui, T.Q., Nguyen, M.N., Zhang, C., 2011. Buckling analysis of Reissner-Mindlin plates subjected to in-plane edge loads using a shear-locking-free and meshfree method. Engineering Analysis with Boundary Elements 35, 1038-1053.

Chikh, A., Tounsi, A., Hebali, H., Mahmoud, S.R., 2017. Thermal buckling analysis of cross-ply laminated plates using a simplified HSDT. Smart Structures and Systems 19, 289-297.

Civalek, Ö., Korkmaz, A., Demir, C., 2010. Discrete singular convolution approach for buckling analysis of rectangular Kirchhoff plates subjected to compressive loads on two-opposite edges. Advances in Engineering Software 41, 557-560.

Civalek, Ö., Yavas, A., 2008. Discrete singular convolution for buckling analyses of plates and columns. Structural Engineering and Mechanics 29, 279-288.

El-Haina, F., Bakora, A., Bousahla, A.A., Tounsi, A., Mahmoud, S.R., 2017. A simple analytical approach for thermal buckling of thick functionally graded sandwich plates. Structural Engineering and Mechanics 63, 585-595.

Jeyaraj, P., 2013. Buckling and free vibration behavior of an isotropic plate under nonuniform thermal load. International Journal of Structural Stability and Dynamics 13.

Kaci, A., Houari, M.S.A., Bousahla, A.A., Tounsi, A., Mahmoud, S.R., 2018. Post-buckling analysis of shear-deformable composite beams using a novel simple two-unknown beam theory. Structural Engineering and Mechanics 65, 621-631.

Komur, M.A., Sonmez, M., 2015. Elastic buckling behavior of rectangular plates with holes subjected to partial edge loading. Journal of Constructional Steel Research 112, 54-60.

Lal, R., Ahlawat, N., 2015. Axisymmetric vibrations and buckling analysis of functionally graded circular plates via differential transform method. European Journal of Mechanics A/Solids 52, 85-94.

Li, D., Smith, S., Ma, X., 2016a. End condition effect on initial buckling performance of thin plates resting on tensionless elastic or rigid foundations. International Journal of Mechanical Sciences 105, 83-89.

Li, R., Ni, X., Cheng, G., 2015a. Symplectic superposition method for benchmark flexure solutions for rectangular thick plates. Journal of Engineering Mechanics 141, 04014119.

Li, R., Tian, Y., Wang, P., Shi, Y., Wang, B., 2016b. New analytic free vibration solutions of rectangular thin plates resting on multiple point supports. International Journal of Mechanical Sciences 110, 53-61.

Li, R., Tian, Y., Zheng, X., Wang, H., Xiong, S., Wang, B., 2017. New analytic bending solutions of rectangular thin plates with a corner point-supported and its adjacent corner free. European Journal of Mechanics A/Solids 66, 103-113.

Li, R., Wang, P., Tian, Y., Wang, B., Li, G., 2015b. A unified analytic solution approach to static bending and free vibration problems of rectangular thin plates. Scientific Reports 5, 17054.

Li, R., Wang, P., Yang, Z., Yang, J., Tong, L., 2018. On new analytic free vibration solutions of rectangular thin cantilever plates in the symplectic space. Applied Mathematical Modelling 53, 310-318.

Lim, C.W., 2010. Symplectic elasticity approach for free vibration of rectangular plates. Advances in Vibration Engineering 9, 159-163.

Lim, C.W., Lu, C.F., Xiang, Y., Yao, W., 2009. On new symplectic elasticity approach for exact free vibration solutions of rectangular kirchhoff plates. International Journal of Engineering Science 47, 131-140.

Lim, C.W., Xu, X.S., 2010. Symplectic elasticity: theory and applications. Applied Mechanics Reviews 63, 050802.

Lopatin, A.V., Morozov, E.V., 2014. Approximate buckling analysis of the CCFF orthotropic plates subjected to in-plane bending. International Journal of Mechanical Sciences 85, 38-44.

Mahi, A., Tounsi, A., 2015. A new hyperbolic shear deformation theory for bending and free vibration analysis of isotropic, functionally graded, sandwich and laminated composite plates. Applied Mathematical Modelling 39, 2489-2508.

Mantari, J.L., Monge, J.C., 2016. Buckling, free vibration and bending analysis of functionally graded sandwich plates based on an optimized hyperbolic unified formulation. International Journal of Mechanical Sciences 119, 170-186.

Menasria, A., Bouhadra, A., Tounsi, A., Bousahla, A.A., Mahmoud, S.R., 2017. A new and simple HSDT for thermal stability analysis of FG sandwich plates. Steel and Composite Structures 25, 157-175.

Meziane, M.A.A., Abdelaziz, H.H., Tounsi, A., 2014. An efficient and simple refined theory for buckling and free vibration of exponentially graded sandwich plates under various boundary conditions. Journal of Sandwich Structures & Materials 16, 293-318.

Mijuskovic, O., Coric, B., Scepanovic, B., 2015. Accurate buckling loads of plates with different boundary conditions under arbitrary edge compression. International Journal of Mechanical Sciences 101, 309-323.

Mirzaei, M., Kiani, Y., 2016. Thermal buckling of temperature dependent FG-CNT reinforced composite plates. Meccanica 51, 2185-2201.

Mohammadi, M., Saidi, A.R., Jomehzadeh, E., 2010. A novel analytical approach for the buckling analysis of moderately thick functionally graded rectangular plates with two simply-supported opposite edges. Proceedings of the Institution of Mechanical Engineers Part C-Journal of Mechanical Engineering Science 224, 1831-1841.

Moradi, S., Taheri, F., 1999. Application of differential quadrature method to the delamination buckling of composite plates. Computers & Structures 70, 615-623.

Moslemi, A., Neya, B.N., Amiri, J.V., 2017. Benchmark solution for buckling of thick rectangular transversely isotropic plates under biaxial load. International Journal of Mechanical Sciences 131, 356-367.

Naderi, A., Saidi, A.R., 2011a. An analytical solution for buckling of moderately thick functionally graded sector and annular sector plates. Archive of Applied Mechanics 81, 809-828.

Naderi, A., Saidi, A.R., 2011b. Exact solution for stability analysis of moderately thick functionally graded sector plates on elastic foundation. Composite Structures 93, 629-638.

Natarajan, S., Chakraborty, S., Ganapathi, M., Subramanian, M., 2014. A parametric study on the buckling of functionally graded material plates with internal discontinuities using the partition of unity method. European Journal of Mechanics A/Solids 44, 136-147.

Ravari, M.R.K., Shahidi, A.R., 2013. Axisymmetric buckling of the circular annular nanoplates using finite difference method. Meccanica 48, 135-144.

Ravari, M.R.K., Talebi, S., Shahidi, A.R., 2014. Analysis of the buckling of rectangular nanoplates by use of finite-difference method. Meccanica 49, 1443-1455.

Wang, B., Li, P., Li, R., 2016. Symplectic superposition method for new analytic buckling solutions of rectangular thin plates. International Journal of Mechanical Sciences 119, 432-441.

Yao, W., Zhong, W., Lim, C.W., 2009. Symplectic Elasticity. World Scientific, Singapore.

Tables

Table 1. First ten buckling load factors, $P_{cr}b^2/(\pi^2 D)$, of uniaxially loaded CCFF plates.

a/*b*	Methods	Modes									
		1st	2nd	3rd	4th	5th	6th	7th	8th	9th	10th
0.4	Present	2.0393	6.6950	14.460	16.805	21.128	31.644	39.202	42.840	44.056	51.562
	FEM	2.0395	6.6963	14.492	16.820	21.161	31.693	39.442	42.980	44.262	51.704
0.6	Present	1.2731	6.1922	7.1549	15.057	17.166	17.737	22.795	31.075	34.194	34.358
	FEM	1.2731	6.1951	7.1594	15.068	17.180	17.784	22.844	31.123	34.255	34.543
0.8	Present	1.0650	4.0624	6.4595	10.210	14.280	16.766	17.938	19.723	25.706	29.817
	FEM	1.0650	4.0642	6.4607	10.225	14.292	16.778	17.961	19.778	25.763	29.857
1	Present	1.0105	2.9500	6.2562	6.8231	12.188	12.631	16.183	16.698	20.601	23.569
	FEM	1.0105	2.9507	6.2577	6.8288	12.195	12.655	16.201	16.712	20.667	23.612
1.5	Present	0.98948	2.1724	3.4416	5.8716	6.3891	9.4529	11.077	11.687	13.830	14.645
	FEM	0.98947	2.1726	3.4428	5.8753	6.3909	9.4655	11.082	11.694	13.858	14.659
2	Present	0.93862	2.0315	2.7356	3.7850	5.6071	6.3081	8.0612	10.397	10.887	11.000
	FEM	0.93860	2.0317	2.7360	3.7863	5.6110	6.3093	8.0701	10.401	10.892	11.017
2.5	Present	0.91392	1.7075	2.4097	3.4205	4.1870	5.4198	6.3255	7.2983	9.4666	10.151
	FEM	0.91390	1.7075	2.4101	3.4213	4.1883	5.4232	6.3268	7.3055	9.4794	10.155
3	Present	0.90996	1.5647	1.9632	2.7735	3.7618	4.7879	5.6052	6.2655	6.8958	8.5440
	FEM	0.90994	1.5648	1.9634	2.7742	3.7633	4.7898	5.6077	6.2670	6.9013	8.5541
3.5	Present	0.90971	1.5396	1.7119	2.2750	2.9960	3.9175	4.9916	5.9813	6.4110	6.9997
	FEM	0.90969	1.5396	1.7120	2.2753	2.9968	3.9192	4.9946	5.9840	6.4163	7.0032
4	Present	0.90916	1.5038	1.6443	1.9932	2.4840	3.1845	4.0104	4.9603	6.0332	6.2826
	FEM	0.90914	1.5038	1.6443	1.9934	2.4845	3.1855	4.0122	4.9633	6.0376	6.2841
4.5	Present	0.90886	1.4506	1.6071	1.9191	2.1654	2.6902	3.3224	4.0753	4.9329	5.8579
	FEM	0.90884	1.4506	1.6072	1.9192	2.1657	2.6909	3.3235	4.0772	4.9359	5.8622
5	Present	0.90881	1.4327	1.5242	1.8441	2.0822	2.3935	2.8430	3.4419	4.1268	4.8945
	FEM	0.90879	1.4328	1.5242	1.8443	2.0823	2.3938	2.8437	3.4431	4.1288	4.8975

Table 2
First ten buckling load factors of uniaxially loaded SSFF plates.

a/*b*	Methods	Modes									
		1st	2nd	3rd	4th	5th	6th	7th	8th	9th	10th
0.4	Present	0.39373	4.7651	6.6099	11.052	15.180	25.156	28.652	29.438	30.600	38.965
	FEM	0.3937	4.7659	6.6158	11.058	15.189	25.254	28.714	29.504	30.652	39.069
0.6	Present	0.40598	3.1245	5.3468	9.2561	11.446	14.573	15.745	25.214	25.716	28.921
	FEM	0.40594	3.1256	5.3474	9.2592	11.466	14.582	15.764	25.312	25.747	28.980
0.8	Present	0.41548	1.9433	5.2125	6.6017	10.326	11.829	14.323	14.758	18.565	23.975
	FEM	0.41545	1.9436	5.2129	6.6077	10.331	11.835	14.350	14.772	18.597	23.998
1	Present	0.42232	1.3960	4.3482	5.1619	8.9316	9.3243	13.252	14.581	14.991	16.382
	FEM	0.42230	1.3961	4.3506	5.1624	8.9348	9.3370	13.263	14.590	15.000	16.422
1.5	Present	0.43227	0.85866	2.1774	4.3660	5.1561	7.4672	8.0852	9.0921	11.439	11.791
	FEM	0.43224	0.85865	2.1778	4.3684	5.1566	7.4751	8.0875	9.0956	11.458	11.800
2	Present	0.43730	0.67360	1.4151	2.6504	4.3753	5.1525	6.6241	7.8881	8.9105	9.3265
	FEM	0.43725	0.67352	1.4152	2.6511	4.3777	5.1513	6.6299	7.8901	8.9135	9.3379
2.5	Present	0.44020	0.58960	1.0636	1.8536	2.9607	4.3810	5.1508	6.1437	7.8771	8.1581
	FEM	0.44018	0.58954	1.0636	1.8538	2.9616	4.3833	5.1473	6.1481	7.8792	8.1623
3	Present	0.44210	0.54490	0.87350	1.4215	2.1899	3.1787	4.3848	5.1508	5.8357	7.4827
	FEM	0.44205	0.54491	0.87352	1.4216	2.1903	3.1798	4.3871	5.1437	5.8385	7.4879
3.5	Present	0.44330	0.51860	0.75950	1.1617	1.7258	2.4523	3.3411	4.3898	5.1398	5.6238
	FEM	0.44333	0.51861	0.75954	1.1617	1.7258	2.4523	3.3411	4.3898	5.1398	5.6238
4	Present	0.44430	0.50210	0.68610	0.99310	1.4241	1.9801	2.6601	3.4641	4.3901	5.1531
	FEM	0.44424	0.50194	0.68599	0.99340	1.4248	1.9805	2.6606	3.4650	4.3918	5.1350
4.5	Present	0.44497	0.49084	0.63595	0.87845	1.2189	1.6575	2.1944	2.8296	3.5633	4.3947
	FEM	0.44491	0.49079	0.63588	0.87838	1.2188	1.6575	2.1944	2.8298	3.5632	4.3934
5	Present	0.44550	0.48310	0.60030	0.79650	1.0719	1.4268	1.8614	2.3758	2.9702	3.6459
	FEM	0.44540	0.48301	0.60025	0.79637	1.0718	1.4267	1.8613	2.3755	2.9695	3.6429

Table 3
First ten buckling load factors of uniaxially loaded CSFF plates with $\kappa = 1$, $\gamma = 0$.

a/*b*	Methods	Modes									
		1st	2nd	3rd	4th	5th	6th	7th	8th	9th	10th
0.4	Present	0.58085	6.0139	6.9798	12.191	17.035	25.222	29.613	31.404	36.969	42.820
	FEM	0.58078	6.0167	6.9847	12.197	17.047	25.321	29.711	31.452	37.047	42.911
0.6	Present	0.71109	3.2230	6.5130	11.388	13.127	15.764	17.263	25.268	28.074	29.734
	FEM	0.71105	3.2240	6.5141	11.406	13.135	15.778	17.280	25.367	28.107	29.833
0.8	Present	0.84515	2.1117	6.1730	6.7835	11.747	14.361	16.384	18.103	19.790	25.297
	FEM	0.84512	2.1120	6.1747	6.7887	11.753	14.391	16.396	18.122	19.815	25.397
1	Present	0.96085	1.6805	4.4448	6.2860	9.4059	10.375	14.198	16.280	16.628	20.889
	FEM	0.96083	1.6805	4.4471	6.2870	9.4185	10.379	14.210	16.316	16.645	20.929
1.5	Present	0.95139	1.8770	2.3496	4.4691	6.2839	7.5683	10.202	11.298	11.576	12.716
	FEM	0.95136	1.8770	2.3500	4.4715	6.2851	7.5761	10.206	11.306	11.592	12.725
2	Present	0.90290	1.6584	2.7147	2.8089	4.4814	6.2511	6.7557	9.4205	9.9766	10.425
	FEM	0.90288	1.6585	2.7148	2.8095	4.4838	6.2526	6.7614	9.4332	9.9802	10.429
2.5	Present	0.90450	1.4287	2.0508	3.0987	3.8421	4.4889	6.1207	6.4087	8.2838	9.8240
	FEM	0.90450	1.4287	2.0510	3.0997	3.8423	4.4913	6.1243	6.4113	8.2935	9.8274
3	Present	0.90970	1.4030	1.6804	2.3652	3.3121	4.4934	5.1998	5.8842	6.3573	7.5710
	FEM	0.90965	1.4030	1.6805	2.3656	3.3132	4.4958	5.2002	5.8885	6.3587	7.5789
3.5	Present	0.90930	1.4439	1.5407	1.9422	2.6142	3.4700	4.4970	5.6782	6.2268	6.9514
	FEM	0.90926	1.4439	1.5407	1.9424	2.6148	3.4713	4.4994	5.6823	6.2282	6.9522
4	Present	0.90870	1.3814	1.6433	1.7191	2.1744	2.8148	3.5930	4.5021	5.5333	6.2584
	FEM	0.90866	1.3814	1.6433	1.7191	2.1744	2.8148	3.5930	4.5021	5.5333	6.2584
4.5	Present	0.90872	1.3605	1.5205	1.8581	1.9185	2.3740	2.9780	3.6895	4.5042	5.4166
	FEM	0.90872	1.3605	1.5205	1.8581	1.9185	2.3740	2.9780	3.6895	4.5042	5.4166
5	Present	0.90880	1.3740	1.4386	1.6845	2.0592	2.1497	2.5447	3.1124	3.7663	4.5034
	FEM	0.90879	1.3740	1.4386	1.6846	2.0595	2.1498	2.5452	3.1134	3.7679	4.5058

Table 4
First ten buckling load factors of uniaxially loaded CSFF plates with $\kappa = 0$, $\gamma = 1$.

a/*b*	Methods	Modes									
		1st	2nd	3rd	4th	5th	6th	7th	8th	9th	10th
0.4	Present	2.9233	4.9338	8.8889	14.834	22.782	31.891	33.122	44.866	51.274	52.690
	FEM	2.9233	4.9338	8.8889	14.834	22.782	31.891	33.122	44.866	51.274	52.690
0.6	Present	1.4078	3.4099	7.3667	13.258	14.375	21.315	24.298	26.072	31.320	33.778
	FEM	1.4078	3.4099	7.3667	13.258	14.375	21.315	24.298	26.072	31.320	33.778
0.8	Present	0.88512	2.8823	6.8251	8.0815	12.816	14.601	18.523	20.795	22.967	26.567
	FEM	0.88512	2.8823	6.8251	8.0815	12.816	14.601	18.523	20.795	22.967	26.567
1	Present	0.64676	2.6382	5.2068	6.6187	10.829	12.508	13.528	14.705	18.412	20.552
	FEM	0.64672	2.6389	5.2073	6.6248	10.836	12.531	13.539	14.714	18.436	20.617
1.5	Present	0.41706	2.2908	2.4931	5.3841	6.3644	6.5919	8.3101	12.321	12.723	13.124
	FEM	0.41704	2.2911	2.4936	5.3853	6.3699	6.5937	8.3164	12.343	12.732	13.131
2	Present	0.34014	1.3426	2.3339	3.6084	3.8588	6.3043	7.2237	7.3842	8.9774	10.468
	FEM	0.34014	1.3425	2.3347	3.6089	3.8593	6.3106	7.2267	7.3889	8.9818	10.474
2.5	Present	0.30591	0.89829	2.2784	2.4472	3.1077	4.7064	5.8881	6.2919	6.9116	7.7442
	FEM	0.30591	0.89824	2.2791	2.4473	3.1085	4.7068	5.8898	6.2981	6.9178	7.7459
3	Present	0.28787	0.67482	1.6931	2.2792	2.8043	3.3280	4.4027	5.4146	6.2630	6.6984
	FEM	0.28788	0.67478	1.6931	2.2801	2.8051	3.3281	4.4038	5.4152	6.2693	6.7046
3.5	Present	0.27725	0.54884	1.2548	2.2599	2.4577	2.6605	3.6638	4.0378	5.9102	6.1384
	FEM	0.27726	0.54882	1.2547	2.2607	2.4578	2.6613	3.6646	4.0380	5.9112	6.1404
4	Present	0.27049	0.47139	0.98086	1.8878	2.2615	2.5464	3.1004	3.2884	4.5779	4.8735
	FEM	0.27050	0.47137	0.98081	1.8878	2.2624	2.5472	3.1005	3.2891	4.5783	4.8747
4.5	Present	0.26592	0.42053	0.80241	1.4966	2.2516	2.4466	2.5150	3.0188	3.6630	4.1259
	FEM	0.26593	0.42052	0.80237	1.4965	2.2525	2.4470	2.5154	3.0196	3.6631	4.1269
5	Present	0.26270	0.38539	0.68109	1.2200	2.0095	2.2543	2.4341	2.8414	3.0061	3.6598
	FEM	0.26271	0.38538	0.68106	1.2199	2.0095	2.2551	2.4349	2.8422	3.0062	3.6607

Table 5
First ten buckling load factors of biaxially loaded CCFF plates with $\kappa = 1$, $\gamma = 1$.

a/*b*	Methods	Modes									
		1st	2nd	3rd	4th	5th	6th	7th	8th	9th	10th
0.4	Present	1.8833	3.6713	6.5383	11.422	13.958	14.107	17.971	19.943	24.120	29.229
	FEM	1.8835	3.6715	6.5417	11.438	13.982	14.136	18.000	19.992	24.171	29.332
0.6	Present	1.0559	2.3455	5.4064	6.0988	8.0403	10.487	12.605	15.656	17.426	18.182
	FEM	1.0559	2.3458	5.4095	6.1041	8.0464	10.497	12.625	15.681	17.468	18.224
0.8	Present	0.75464	1.7918	3.6606	4.6607	6.4791	8.1831	9.6797	11.071	12.124	13.482
	FEM	0.75460	1.7921	3.6623	4.6622	6.4843	8.1882	9.6935	11.084	12.143	13.498
1	Present	0.59800	1.4561	2.7454	3.8342	5.6991	6.5342	6.8499	8.6032	10.815	11.355
	FEM	0.59797	1.4564	2.7462	3.835	5.703	6.540	6.854	8.610	10.824	11.375
1.5	Present	0.41254	0.94019	2.1897	2.3390	3.2390	4.3067	5.3511	6.0296	6.6454	6.9871
	FEM	0.41252	0.94022	2.1903	2.3395	3.2400	4.3078	5.3549	6.0347	6.6503	6.9917
2	Present	0.33667	0.71184	1.4604	2.1360	2.5002	2.8712	3.5870	4.5776	5.0921	6.0480
	FEM	0.33667	0.71182	1.4606	2.1367	2.5008	2.8720	3.5880	4.5792	5.0954	6.0524
2.5	Present	0.30133	0.58741	1.0461	1.8275	2.2334	2.2571	2.8754	3.1909	3.8593	4.6766
	FEM	0.30133	0.58739	1.0462	1.8278	2.2339	2.2578	2.8760	3.1920	3.8603	4.6789
3	Present	0.28311	0.50411	0.82717	1.3746	2.0078	2.2190	2.3945	2.5193	3.1943	3.3921
	FEM	0.28311	0.50408	0.82717	1.3747	2.0083	2.2198	2.3951	2.5198	3.1950	3.3934
3.5	Present	0.27281	0.44419	0.69724	1.0859	1.6407	2.1566	2.2079	2.2682	2.6220	2.8020
	FEM	0.27281	0.44417	0.69722	1.0859	1.6410	2.1572	2.2085	2.2688	2.6227	2.8025
4	Present	0.26651	0.40073	0.61002	0.90129	1.3283	1.8573	2.1416	2.2278	2.3230	2.4765
	FEM	0.26652	0.40072	0.61000	0.90129	1.3284	1.8576	2.1422	2.2286	2.3236	2.4770
4.5	Present	0.26242	0.36912	0.54573	0.77720	1.1080	1.5421	2.0085	2.2097	2.2142	2.2357
	FEM	0.26243	0.36911	0.54570	0.77718	1.1080	1.5423	2.0090	2.2103	2.2149	2.2365
5	Present	0.25962	0.34588	0.49586	0.68887	0.95133	1.3021	1.7248	2.0986	2.1777	2.2218
	FEM	0.25963	0.34588	0.49584	0.68885	0.95134	1.3022	1.7250	2.0991	2.1784	2.2226

Table 6
First ten buckling load factors of biaxially loaded CCFF plates with $\kappa = 1$, $\gamma = 5$.

a/*b*	Methods	Modes									
		1st	2nd	3rd	4th	5th	6th	7th	8th	9th	10th
0.4	Present	1.0510	1.4150	1.9250	2.9640	4.5150	6.3500	7.0180	8.6100	9.1150	9.2510
	FEM	1.0514	1.4153	1.9255	2.9681	4.5272	6.3753	7.0356	8.6447	9.1449	9.2785
0.6	Present	0.48680	0.72480	1.4813	2.5554	3.1037	4.0749	4.2839	4.5561	5.0658	6.2625
	FEM	0.48681	0.72483	1.4824	2.5595	3.1063	4.0811	4.2930	4.5622	5.0722	6.2907
0.8	Present	0.27610	0.55400	1.3500	1.7478	2.2468	2.6581	2.7626	3.7466	4.1225	4.6151
	FEM	0.27611	0.55408	1.3511	1.7485	2.2488	2.6611	2.7651	3.7513	4.1353	4.6213
1	Present	0.18278	0.49182	1.1211	1.3189	1.5151	2.1126	2.5177	2.9238	3.2591	4.0663
	FEM	0.18278	0.49192	1.1213	1.3200	1.5156	2.1138	2.5223	2.9262	3.2635	4.0783
1.5	Present	0.099555	0.41799	0.54759	0.80759	1.2584	1.3308	1.6026	2.0247	2.3257	2.4582
	FEM	0.099552	0.41807	0.54767	0.80771	1.2595	1.3313	1.6037	2.0257	2.3270	2.4628
2	Present	0.074479	0.27866	0.46016	0.59415	0.79067	1.1531	1.2636	1.4116	1.4622	1.8295
	FEM	0.074479	0.27865	0.46030	0.59423	0.79076	1.1534	1.2648	1.4124	1.4629	1.8307
2.5	Present	0.064213	0.18983	0.43193	0.46739	0.59073	0.80525	0.97097	1.2500	1.3450	1.4166
	FEM	0.064213	0.18983	0.43200	0.46750	0.59084	0.80536	0.97112	1.2513	1.3460	1.4172
3	Present	0.059167	0.14227	0.32443	0.44726	0.52683	0.60545	0.74734	0.98427	1.1410	1.2483
	FEM	0.059168	0.14226	0.32443	0.44742	0.52695	0.60551	0.74746	0.98442	1.1413	1.2495
3.5	Present	0.056357	0.11472	0.24558	0.42985	0.46944	0.50414	0.63962	0.74115	0.90427	1.0996
	FEM	0.056358	0.11472	0.24557	0.42993	0.46953	0.50427	0.63974	0.74121	0.90444	1.0998
4	Present	0.054645	0.097611	0.19434	0.35037	0.44767	0.48280	0.56944	0.59359	0.76512	0.85237
	FEM	0.054646	0.097608	0.19433	0.35036	0.44783	0.48293	0.56951	0.59368	0.76526	0.85245
4.5	Present	0.053529	0.086366	0.16005	0.28192	0.43237	0.45622	0.49146	0.54662	0.66978	0.69271
	FEM	0.053531	0.086364	0.16005	0.28191	0.43245	0.45634	0.49158	0.54674	0.66987	0.69280
5	Present	0.052763	0.078626	0.13630	0.23252	0.36672	0.44577	0.47408	0.51285	0.56674	0.62475
	FEM	0.052765	0.078625	0.13629	0.23251	0.36671	0.44593	0.47423	0.51294	0.56681	0.62487

Table 7
First ten buckling load factors of biaxially loaded SSFF plates with $\kappa = 1$, $\gamma = 1$.

a/*b*	Methods	Modes									
		1st	2nd	3rd	4th	5th	6th	7th	8th	9th	10th
0.4	Present	0.34749	2.1334	4.7288	6.5060	8.4314	9.9459	13.114	16.586	19.099	24.454
	FEM	0.34744	2.1334	4.7309	6.5121	8.4380	9.9572	13.127	16.623	19.128	24.544
0.6	Present	0.31013	1.5311	2.9614	4.2154	5.3607	8.6190	9.4085	11.220	12.878	14.159
	FEM	0.31011	1.5312	2.9625	4.2171	5.3629	8.6250	9.4200	11.239	12.896	14.177
0.8	Present	0.26398	1.2025	1.8740	3.6011	4.3555	6.2107	6.9825	8.2802	9.2503	11.451
	FEM	0.26396	1.2026	1.8744	3.6018	4.3577	6.2157	6.9866	8.2871	9.2624	11.462
1	Present	0.21804	0.98165	1.4206	2.9538	3.9133	4.3390	5.5776	6.4248	8.8135	8.9938
	FEM	0.21802	0.98170	1.4208	2.9541	3.9154	4.3416	5.5797	6.4282	8.8254	9.0032
1.5	Present	0.13122	0.62266	1.1056	1.7862	2.1704	3.5152	3.9229	4.2338	4.9082	5.7874
	FEM	0.13121	0.62265	1.1057	1.7864	2.1707	3.5159	3.9252	4.2363	4.9106	5.7900
2	Present	0.082621	0.44656	0.98472	1.1738	1.6222	2.3172	2.6800	3.8248	3.9575	4.1900
	FEM	0.082616	0.44654	0.98482	1.1740	1.6223	2.3178	2.6804	3.8262	3.9595	4.1924
2.5	Present	0.055598	0.34134	0.75661	1.0410	1.3490	1.5913	2.0982	2.6538	3.0558	3.9127
	FEM	0.055594	0.34132	0.75663	1.0411	1.3491	1.5916	2.0984	2.6547	3.0563	3.9148
3	Present	0.039620	0.26813	0.58460	0.98927	1.1125	1.2964	1.7282	1.9357	2.4798	2.8810
	FEM	0.039617	0.26811	0.58459	0.98939	1.1126	1.2966	1.7284	1.9361	2.4801	2.8821
3.5	Present	0.029543	0.21418	0.47204	0.83121	1.0237	1.1852	1.4014	1.5996	2.0529	2.2171
	FEM	0.029541	0.21417	0.47203	0.83125	1.0239	1.1853	1.4015	1.5998	2.0532	2.2176
4	Present	0.022828	0.17366	0.39210	0.67863	0.99275	1.0823	1.1829	1.4303	1.6633	1.8858
	FEM	0.022827	0.17365	0.39208	0.67864	0.99288	1.0824	1.1830	1.4305	1.6636	1.8860
4.5	Present	0.018147	0.14286	0.33138	0.56778	0.87758	1.0169	1.1139	1.2901	1.3959	1.6795
	FEM	0.018146	0.14285	0.33137	0.56778	0.87763	1.0170	1.1140	1.2902	1.3961	1.6796
5	Present	0.014761	0.11914	0.28334	0.48512	0.74461	0.99524	1.0617	1.1345	1.2804	1.4998
	FEM	0.014760	0.11914	0.28333	0.48511	0.74464	0.99538	1.0619	1.1346	1.2805	1.4999

Table 8
First ten buckling load factors of biaxially loaded SSFF plates with $\kappa = 1$, $\gamma = 5$.

a/b	Methods	Modes									
		1st	2nd	3rd	4th	5th	6th	7th	8th	9th	10th
0.4	Present	0.23500	0.62000	1.2210	2.2200	3.5970	5.0900	5.5240	5.8590	6.0890	6.9710
	FEM	0.23539	0.62043	1.2212	2.2224	3.6052	5.0991	5.5388	5.8660	6.0966	6.9805
0.6	Present	0.15600	0.38300	0.98000	1.9450	2.3410	2.5930	3.0740	3.3870	4.0220	5.1560
	FEM	0.15627	0.38300	0.98085	1.9473	2.3421	2.5945	3.0755	3.3949	4.0255	5.1758
0.8	Present	0.10400	0.30000	0.88800	1.3000	1.4990	1.9030	2.0490	3.0080	3.2830	3.9290
	FEM	0.10378	0.29957	0.88865	1.3003	1.4990	1.9058	2.0501	3.0110	3.2912	3.9323
1	Present	0.071635	0.26119	0.78553	0.90092	1.0112	1.5790	1.8557	2.4594	2.6310	3.2432
	FEM	0.071630	0.26120	0.78572	0.90130	1.0114	1.5795	1.8582	2.4612	2.6334	3.2512
1.5	Present	0.033826	0.22191	0.36684	0.54190	0.82266	1.0853	1.1767	1.5098	1.8115	1.8581
	FEM	0.033824	0.22193	0.36685	0.54192	0.82315	1.0856	1.1771	1.5103	1.8137	1.8592
2	Present	0.019203	0.18934	0.22552	0.38489	0.63544	0.80595	0.85843	0.99367	1.2542	1.3842
	FEM	0.019202	0.18934	0.22554	0.38490	0.63549	0.80639	0.85863	0.99415	1.2545	1.3848
2.5	Present	0.012273	0.12504	0.20853	0.31211	0.40985	0.58589	0.79599	0.82556	0.92083	1.1248
	FEM	0.012273	0.12504	0.20856	0.31212	0.40986	0.58594	0.79635	0.82579	0.92131	1.1252
3	Present	0.0084959	0.085710	0.20308	0.25972	0.29752	0.45286	0.57595	0.78760	0.81770	0.88395
	FEM	0.0084954	0.085705	0.20311	0.25972	0.29754	0.45288	0.57597	0.78791	0.81803	0.88442
3.5	Present	0.0062224	0.061968	0.18748	0.20847	0.26181	0.37321	0.43018	0.61120	0.70619	0.80074
	FEM	0.0062221	0.061964	0.18748	0.20849	0.26183	0.37323	0.43020	0.61126	0.70624	0.80124
4	Present	0.0047516	0.046732	0.14446	0.20212	0.24462	0.30653	0.34975	0.49332	0.55123	0.76315
	FEM	0.0047513	0.046729	0.14445	0.20215	0.24464	0.30653	0.34977	0.49335	0.55126	0.76330
4.5	Present	0.0037464	0.036436	0.11224	0.19971	0.22951	0.24855	0.31108	0.40855	0.45095	0.61557
	FEM	0.0037462	0.036434	0.11224	0.19974	0.22952	0.24856	0.31110	0.40856	0.45097	0.61562
5	Present	0.0030294	0.029179	0.089287	0.18701	0.20374	0.23000	0.28640	0.33732	0.39072	0.50695
	FEM	0.0030293	0.029178	0.089283	0.18702	0.20376	0.23003	0.28642	0.33733	0.39074	0.50697

Table 9
First ten buckling load factors of biaxially loaded CSFF plates with $\kappa = 1$, $\gamma = 1$.

a/*b*	Methods	Modes 1st	2nd	3rd	4th	5th	6th	7th	8th	9th	10th
0.4	Present	0.50086	2.6272	5.8185	6.6464	9.3018	11.619	14.468	19.124	21.033	24.949
	FEM	0.50081	2.6276	5.8223	6.6524	9.3092	11.635	14.486	19.166	21.081	25.045
0.6	Present	0.50481	1.9436	3.2728	5.0851	6.6032	9.5574	10.958	12.174	13.609	15.339
	FEM	0.50477	1.9439	3.2740	5.0870	6.6081	9.5639	10.976	12.195	13.629	15.359
0.8	Present	0.47033	1.4899	2.3990	4.1449	5.9440	6.5355	7.6548	9.2172	11.580	12.768
	FEM	0.47030	1.4901	2.3996	4.1458	5.9490	6.5415	7.6594	9.2247	11.597	12.785
1	Present	0.42640	1.1615	2.1627	3.3722	4.3147	5.7048	6.4827	7.5580	9.0667	10.133
	FEM	0.42638	1.1616	2.1633	3.3728	4.3170	5.7082	6.4875	7.5633	9.0788	10.141
1.5	Present	0.34552	0.77591	1.7799	2.2118	2.7116	3.8893	4.3413	5.7524	6.3011	6.6981
	FEM	0.34551	0.77589	1.7802	2.2125	2.7121	3.8904	4.3433	5.7557	6.3065	6.7032
2	Present	0.30544	0.61728	1.1840	2.0785	2.2363	2.5461	3.1926	4.1030	4.4677	5.7757
	FEM	0.30544	0.61725	1.1840	2.0790	2.2369	2.5468	3.1932	4.1050	4.4691	5.7790
2.5	Present	0.28519	0.52228	0.890865	1.5597	2.1728	2.2022	2.5650	2.8788	3.5495	4.1606
	FEM	0.28520	0.52225	0.89087	1.5599	2.1735	2.2029	2.5655	2.8795	3.5502	4.1628
3	Present	0.27398	0.45605	0.731998	1.1871	1.8465	2.1784	2.2187	2.4443	2.8629	3.1478
	FEM	0.27399	0.45603	0.73198	1.1872	1.8468	2.1790	2.2195	2.4448	2.8636	3.1486
3.5	Present	0.26723	0.40861	0.631986	0.95978	1.4578	2.0358	2.1819	2.2389	2.3681	2.7148
	FEM	0.26724	0.40859	0.63196	0.95979	1.4580	2.0363	2.1826	2.2396	2.3686	2.7153
4	Present	0.26289	0.37446	0.560981	0.81353	1.1890	1.6874	2.1242	2.1918	2.2274	2.3870
	FEM	0.26290	0.37444	0.56096	0.81353	1.1891	1.6877	2.1248	2.1924	2.2281	2.3876
4.5	Present	0.25995	0.34960	0.50697	0.71318	1.0041	1.4002	1.8750	2.1554	2.1878	2.2288
	FEM	0.25996	0.34959	0.50695	0.71316	1.0041	1.4003	1.8753	2.1561	2.1884	2.2296
5	Present	0.25787	0.33119	0.46464	0.63972	0.87280	1.1901	1.5876	2.0181	2.1608	2.1933
	FEM	0.25788	0.33118	0.46462	0.63970	0.87280	1.1902	1.5878	2.0186	2.1614	2.1939

Table 10
First ten buckling load factors of biaxially loaded CSFF plates with $\kappa = 1$, $\gamma = 5$.

a/*b*	Methods	Modes									
		1st	2nd	3rd	4th	5th	6th	7th	8th	9th	10th
0.4	Present	0.31573	0.74033	1.5981	2.7649	4.3521	5.2159	5.8417	6.2799	6.4892	7.3926
	FEM	0.31571	0.74038	1.5991	2.7693	4.3640	5.2240	5.8503	6.2878	6.5153	7.4043
0.6	Present	0.21630	0.54730	1.3913	2.2465	2.5545	2.7718	3.3641	4.1830	4.5080	6.0432
	FEM	0.21623	0.54740	1.3924	2.2481	2.5572	2.7747	3.3663	4.1958	4.5135	6.0568
0.8	Present	0.15330	0.49240	1.2632	1.3608	1.6078	2.3861	2.5225	3.5138	3.9377	4.1330
	FEM	0.15329	0.49252	1.2637	1.3617	1.6082	2.3874	2.5272	3.5183	3.9430	4.1459
1	Present	0.11817	0.46714	0.84043	1.1450	1.2956	1.9448	2.4470	2.5596	3.0822	3.6434
	FEM	0.11816	0.46725	0.84054	1.1451	1.2968	1.9459	2.4506	2.5623	3.0864	3.6464
1.5	Present	0.080186	0.36672	0.47229	0.71591	1.1323	1.2684	1.5381	1.6112	2.1663	2.3019
	FEM	0.080183	0.36672	0.47242	0.71601	1.1325	1.2696	1.5392	1.6118	2.1674	2.3033
2	Present	0.066533	0.22702	0.44865	0.56291	0.67143	1.0087	1.2455	1.2899	1.4098	1.7567
	FEM	0.066533	0.22701	0.44879	0.56299	0.67151	1.0089	1.2465	1.2905	1.4110	1.7579
2.5	Present	0.060311	0.15985	0.39141	0.45701	0.54356	0.75105	0.85462	1.2410	1.2847	1.3413
	FEM	0.060311	0.15984	0.39143	0.45716	0.54368	0.75116	0.85473	1.2420	1.2853	1.3424
3	Present	0.056999	0.12408	0.28442	0.44531	0.50097	0.57032	0.67722	0.92625	1.0129	1.2473
	FEM	0.057000	0.12408	0.28441	0.44546	0.50109	0.57038	0.67734	0.92639	1.0131	1.2486
3.5	Present	0.055040	0.10307	0.21699	0.40334	0.45281	0.49670	0.59803	0.70195	0.82196	1.0449
	FEM	0.055041	0.10307	0.21698	0.40336	0.45296	0.49683	0.59815	0.70202	0.82210	1.0451
4	Present	0.053789	0.089793	0.17404	0.31818	0.44439	0.47824	0.52683	0.57720	0.71024	0.81265
	FEM	0.053791	0.089790	0.17403	0.31817	0.44455	0.47838	0.52690	0.57731	0.71036	0.81274
4.5	Present	0.052943	0.080903	0.14539	0.25647	0.41046	0.45112	0.47763	0.53681	0.62152	0.67101
	FEM	0.052945	0.080901	0.14538	0.25646	0.41049	0.45126	0.47777	0.53694	0.62159	0.67112
5	Present	0.052345	0.074676	0.12546	0.21280	0.34014	0.44409	0.46761	0.50288	0.53382	0.60908
	FEM	0.052348	0.074675	0.12546	0.21279	0.34013	0.44424	0.46776	0.50297	0.53392	0.60920

Table 11
Convergence study for CCFF plates with $\kappa = 1$, $\gamma = 0$.

a/b	Number of series terms	Modes									
		1st	2nd	3rd	4th	5th	6th	7th	8th	9th	10th
0.4	10	2.0391	6.6995	14.460	16.824	21.128	31.690	39.201	42.835	44.059	51.647
	80	**2.0393**	**6.6950**	**14.460**	**16.805**	**21.128**	**31.644**	**39.202**	**42.840**	**44.056**	**51.562**
	90	2.0393	6.6950	14.460	16.805	21.128	31.644	39.202	42.840	44.056	51.562
4.5	10	0.90442	1.4498	1.6068	1.9164	2.1654	2.6880	3.3216	4.0709	4.9220	5.7604
	70	**0.90886**	**1.4506**	**1.6071**	**1.9191**	**2.1654**	**2.6902**	**3.3224**	**4.0753**	**4.9329**	**5.8579**
	80	0.90886	1.4506	1.6071	1.9191	2.1654	2.6902	3.3224	4.0753	4.9329	5.8579

Table 12
Convergence study for SSFF plates with $\kappa = 1$, $\gamma = 0$.

a/*b*	Number of series terms	Modes									
		1st	2nd	3rd	4th	5th	6th	7th	8th	9th	10th
0.4	10	0.39373	4.7652	6.6099	11.052	15.180	25.156	28.652	29.439	30.600	38.965
	40	**0.39373**	**4.7651**	**6.6099**	**11.052**	**15.180**	**25.156**	**28.652**	**29.438**	**30.600**	**38.965**
	50	0.39373	4.7651	6.6099	11.052	15.180	25.156	28.652	29.438	30.600	38.965
4.5	10	0.44497	0.49084	0.63594	0.87845	1.2189	1.6575	2.1944	2.8296	3.5633	4.3947
	30	**0.44497**	**0.49084**	**0.63595**	**0.87845**	**1.2189**	**1.6575**	**2.1944**	**2.8296**	**3.5633**	**4.3947**
	40	0.44497	0.49084	0.63595	0.87845	1.2189	1.6575	2.1944	2.8296	3.5633	4.3947

Table 13
Convergence study for CSFF plates with $\kappa = 1$, $\gamma = 0$.

a/*b*	Number of series terms	Modes									
		1st	2nd	3rd	4th	5th	6th	7th	8th	9th	10th
0.4	10	0.58103	6.0172	6.9808	12.192	17.052	25.222	29.613	31.449	36.972	42.818
	80	**0.58085**	**6.0139**	**6.9798**	**12.191**	**17.035**	**25.222**	**29.613**	**31.404**	**36.969**	**42.820**
	90	0.58085	6.0139	6.9798	12.191	17.035	25.222	29.613	31.404	36.969	42.820
4.5	10	0.90430	1.3602	1.5192	1.8576	1.9161	2.3704	2.9730	3.6816	4.4885	5.3491
	70	**0.90872**	**1.3605**	**1.5205**	**1.8581**	**1.9185**	**2.3740**	**2.9780**	**3.6895**	**4.5042**	**5.4166**
	80	0.90872	1.3605	1.5205	1.8581	1.9185	2.3740	2.9780	3.6895	4.5042	5.4166

Table 14
Convergence study for CSFF plates with $\kappa = 0$, $\gamma = 1$.

a/*b*	Number of series terms	Modes									
		1st	2nd	3rd	4th	5th	6th	7th	8th	9th	10th
0.4	10	2.9235	4.9338	8.8842	14.814	22.722	31.830	33.025	44.597	51.173	52.583
	30	**2.9233**	**4.9338**	**8.8889**	**14.834**	**22.782**	**31.891**	**33.122**	**44.866**	**51.274**	**52.690**
	40	2.9233	4.9338	8.8889	14.834	22.782	31.891	33.122	44.866	51.274	52.690
4.5	10	0.26582	0.42049	0.80241	1.4965	2.2516	2.4465	2.5150	3.0184	3.6633	4.1247
	70	**0.26592**	**0.42053**	**0.80241**	**1.4966**	**2.2516**	**2.4466**	**2.5150**	**3.0188**	**3.6630**	**4.1259**
	80	0.26592	0.42053	0.80241	1.4966	2.2516	2.4466	2.5150	3.0188	3.6630	4.1259

Table 15
Convergence study for CCFF plates with $\kappa = 1,\ \gamma = 1$.

a/*b*	Number of series terms	Modes									
		1st	2nd	3rd	4th	5th	6th	7th	8th	9th	10th
0.4	10	1.8831	3.6721	6.5386	11.426	13.964	14.103	17.970	19.952	24.113	29.239
	70	**1.8833**	**3.6713**	**6.5383**	**11.422**	**13.958**	**14.107**	**17.971**	**19.943**	**24.120**	**29.229**
	80	1.8833	3.6713	6.5383	11.422	13.958	14.107	17.971	19.943	24.120	29.229
4.5	10	0.26231	0.36927	0.54568	0.77642	1.1069	1.5419	2.0094	2.2102	2.2139	2.2355
	70	**0.26242**	**0.36912**	**0.54573**	**0.77720**	**1.1080**	**1.5421**	**2.0085**	**2.2097**	**2.2142**	**2.2357**
	80	0.26242	0.36912	0.54573	0.77719	1.1080	1.5421	2.0085	2.2097	2.2142	2.2357

Table 16
Convergence study for CCFF plates with $\kappa = 1$, $\gamma = 5$.

a/*b*	Number of series terms	Modes									
		1st	2nd	3rd	4th	5th	6th	7th	8th	9th	10th
0.4	10	1.0512	1.4144	1.9247	2.9638	4.5151	6.3445	7.0024	8.6125	9.1108	9.2506
	70	**1.0510**	**1.4150**	**1.9250**	**2.9640**	**4.5150**	**6.3500**	**7.0180**	**8.6100**	**9.1150**	**9.2510**
	80	1.0510	1.4150	1.9250	2.9640	4.5150	6.3500	7.0180	8.6100	9.1150	9.2510
4.5	10	0.053510	0.086411	0.16021	0.28233	0.43261	0.45647	0.49170	0.54654	0.67016	0.69369
	70	**0.053529**	**0.086366**	**0.16005**	**0.28192**	**0.43237**	**0.45622**	**0.49146**	**0.54662**	**0.66978**	**0.69271**
	80	0.053529	0.086366	0.16005	0.28192	0.43237	0.45622	0.49146	0.54662	0.66978	0.69271

Table 17
Convergence study for SSFF plates with $\kappa = 1$, $\gamma = 1$.

a/*b*	Number of series terms	Modes									
		1st	2nd	3rd	4th	5th	6th	7th	8th	9th	10th
0.4	10	0.34749	2.1334	4.7289	6.5060	8.4314	9.9462	13.115	16.587	19.101	24.455
	20	**0.34749**	**2.1334**	**4.7288**	**6.5060**	**8.4314**	**9.9459**	**13.114**	**16.586**	**19.099**	**24.454**
	30	0.34749	2.1333	4.7288	6.5060	8.4313	9.9459	13.114	16.586	19.099	24.454
4.5	10	0.018147	0.14286	0.33141	0.56784	0.87765	1.0169	1.1139	1.2901	1.3961	1.6796
	30	**0.018147**	**0.14286**	**0.33138**	**0.56778**	**0.87758**	**1.0169**	**1.1139**	**1.2901**	**1.3959**	**1.6795**
	40	0.018147	0.14286	0.33138	0.56778	0.87758	1.0169	1.1139	1.2901	1.3959	1.6795

Table 18
Convergence study for SSFF plates with $\kappa = 1$, $\gamma = 5$.

a/*b*	Number of series terms	Modes 1st	2nd	3rd	4th	5th	6th	7th	8th	9th	10th
0.4	10	0.23541	0.62045	1.2208	2.2199	3.5973	5.0899	5.5239	5.8591	6.0893	6.9709
	30	**0.23500**	**0.62000**	**1.2210**	**2.2200**	**3.5970**	**5.0900**	**5.5240**	**5.8590**	**6.0890**	**6.9710**
	40	0.23500	0.62000	1.2210	2.2200	3.5970	5.0900	5.5240	5.8590	6.0890	6.9710
4.5	10	0.0037464	0.036436	0.11224	0.19971	0.22951	0.24856	0.31108	0.40858	0.45096	0.61565
	20	**0.0037464**	**0.036436**	**0.11224**	**0.19971**	**0.22951**	**0.24855**	**0.31108**	**0.40855**	**0.45095**	**0.61557**
	30	0.0037464	0.036436	0.11224	0.19971	0.22951	0.24855	0.31108	0.40855	0.45095	0.61557

Table 19
Convergence study for CSFF plates with $\kappa = 1$, $\gamma = 1$.

a/*b*	Number of series terms	Modes									
		1st	2nd	3rd	4th	5th	6th	7th	8th	9th	10th
0.4	10	0.50099	2.6279	5.8200	6.6478	9.3024	11.628	14.470	19.143	21.036	24.949
	50	**0.50086**	**2.6272**	**5.8185**	**6.6464**	**9.3018**	**11.619**	**14.468**	**19.124**	**21.033**	**24.949**
	60	0.50086	2.6272	5.8185	6.6464	9.3018	11.619	14.468	19.124	21.033	24.949
4.5	10	0.25983	0.34958	0.50680	0.71204	1.0021	1.3978	1.8722	2.1553	2.1879	2.2286
	70	**0.25995**	**0.34960**	**0.50697**	**0.71318**	**1.0041**	**1.4002**	**1.8750**	**2.1554**	**2.1878**	**2.2288**
	80	0.25995	0.34960	0.50697	0.71318	1.0041	1.4002	1.8750	2.1554	2.1878	2.2288

Table 20
Convergence study for CSFF plates with $\kappa = 1$, $\gamma = 5$.

a/*b*	Number of series terms	Modes									
		1st	2nd	3rd	4th	5th	6th	7th	8th	9th	10th
0.4	10	0.31578	0.74045	1.5984	2.7657	4.3533	5.2178	5.8429	6.2813	6.4920	7.3952
	50	**0.31573**	**0.74033**	**1.5981**	**2.7649**	**4.3521**	**5.2159**	**5.8417**	**6.2799**	**6.4892**	**7.3926**
	60	0.31573	0.74033	1.5981	2.7649	4.3521	5.2159	5.8417	6.2799	6.4892	7.3926
4.5	10	0.052922	0.080896	0.14539	0.25643	0.41030	0.45111	0.47759	0.53656	0.62127	0.67079
	80	**0.052943**	**0.080903**	**0.14539**	**0.25647**	**0.41046**	**0.45112**	**0.47763**	**0.53681**	**0.62152**	**0.67101**
	90	0.052943	0.080903	0.14539	0.25647	0.41046	0.45112	0.47763	0.53681	0.62152	0.67101

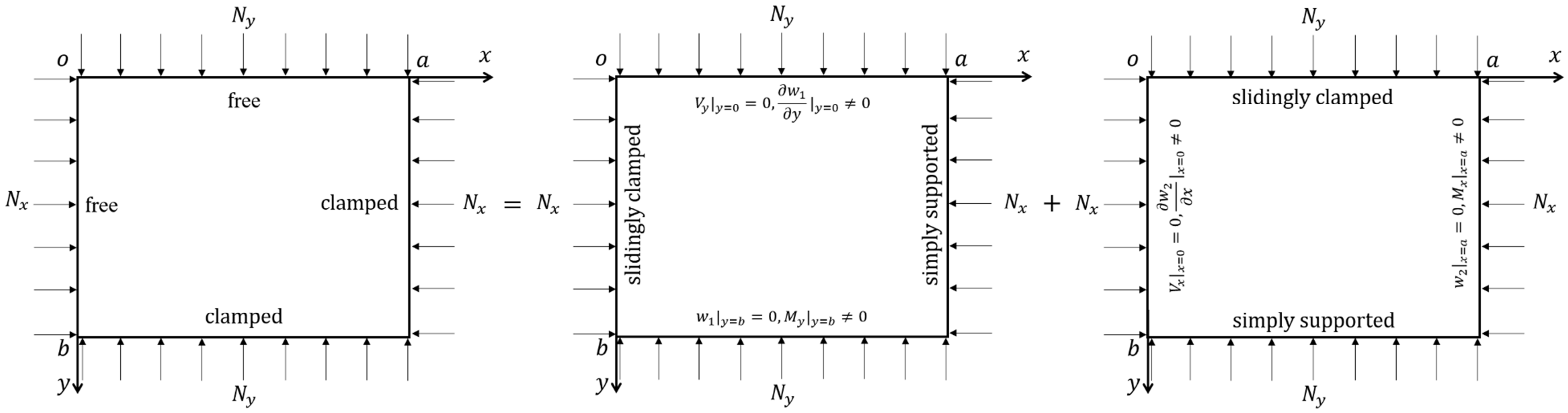

(a) **(b)** **(c)**

Fig. 1. Symplectic superposition method for buckling of a CCFF plate.

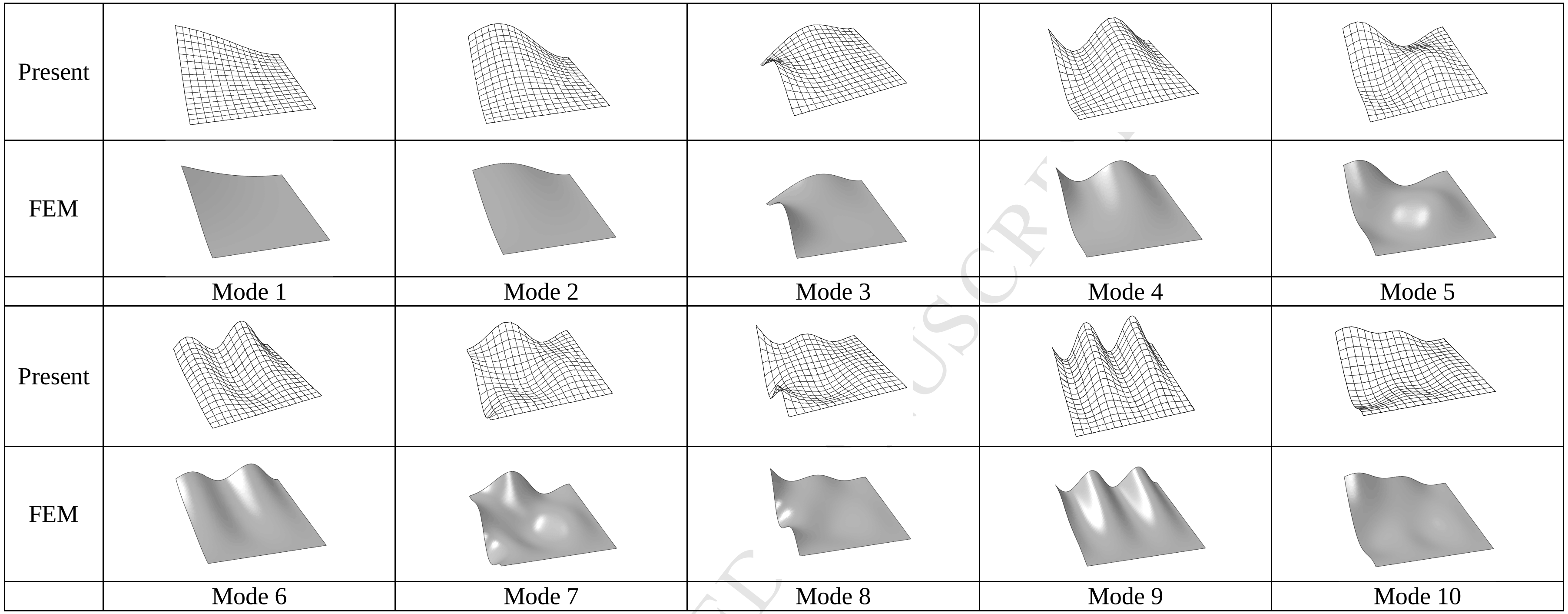

Fig. 2. First ten buckling modes of a uniaxially loaded CCFF square plate.

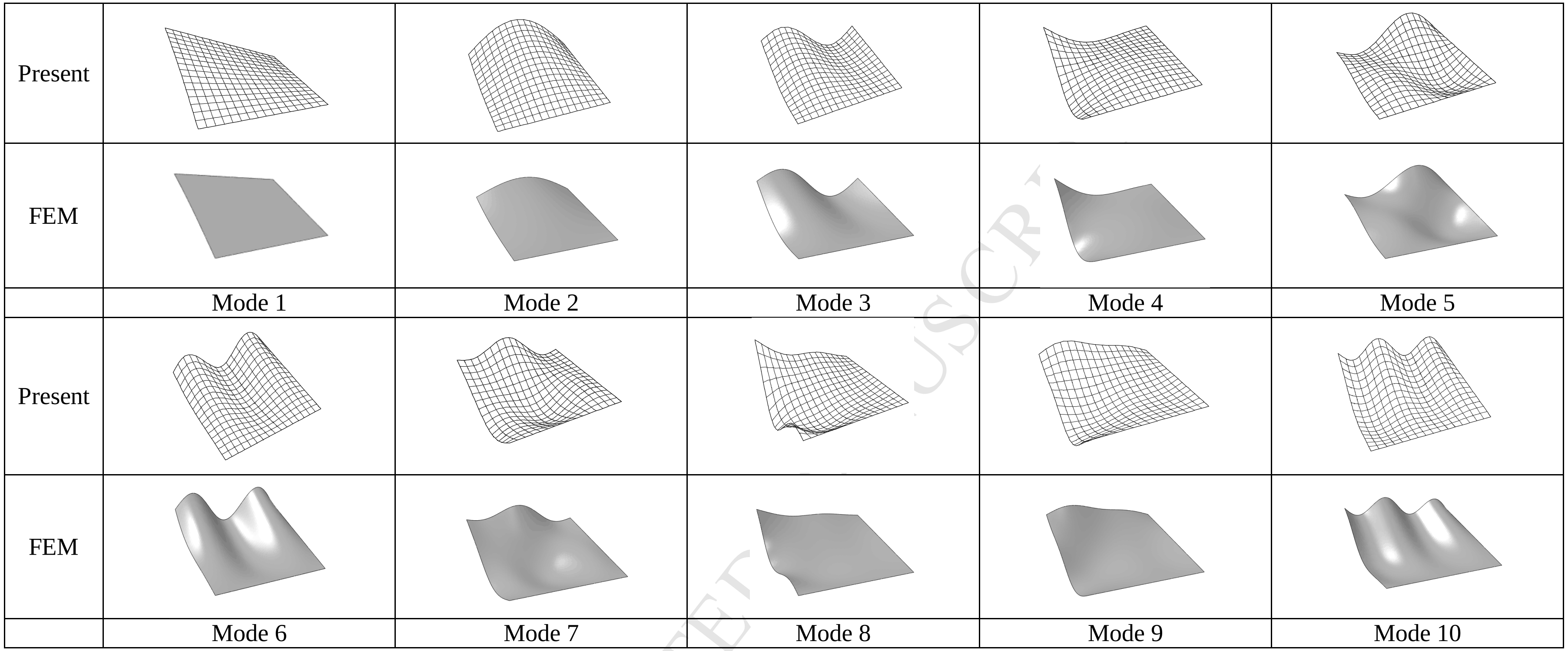

Fig. 3. First ten buckling modes of a uniaxially loaded SSFF square plate.

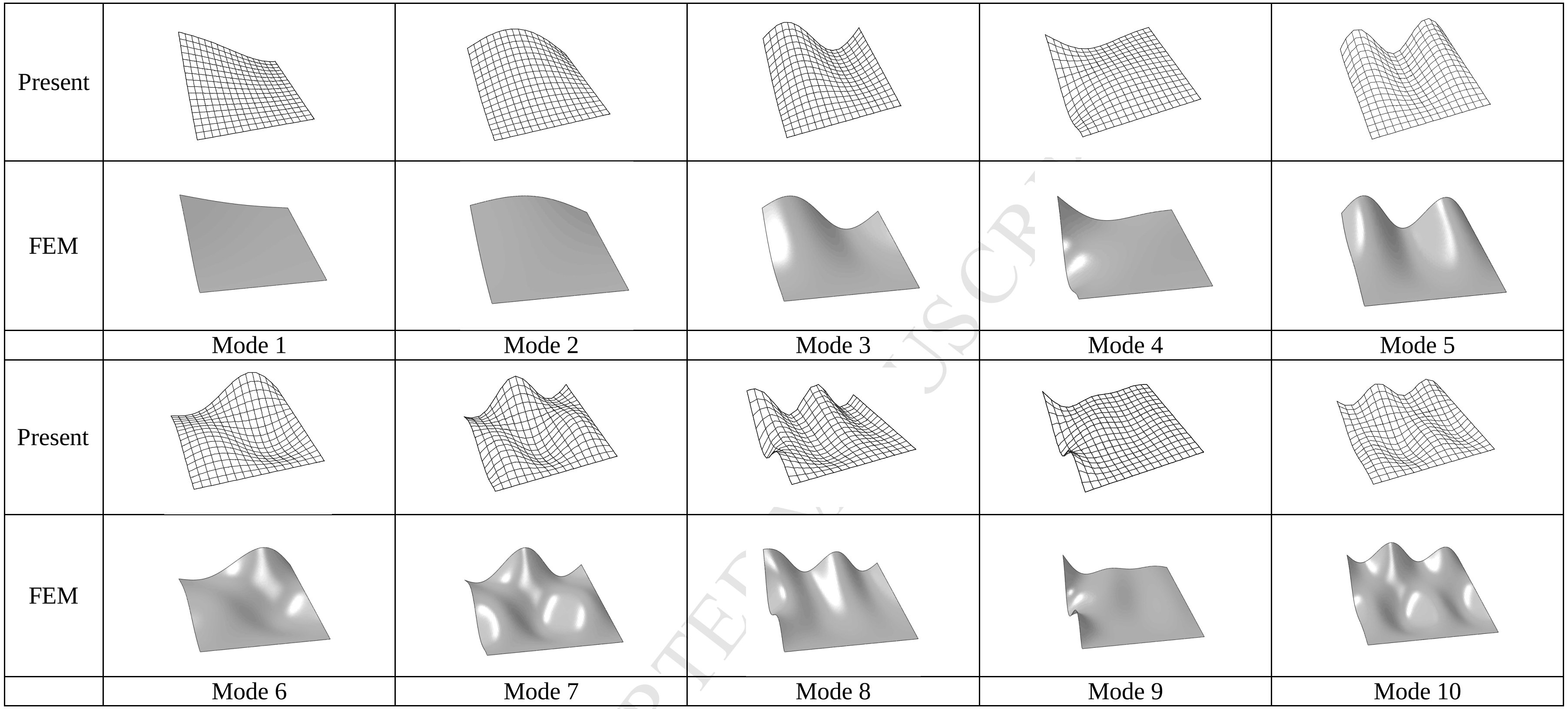

Fig. 4. First ten buckling modes of a uniaxially loaded CSFF square plate with $\kappa = 1$, $\gamma = 0$.

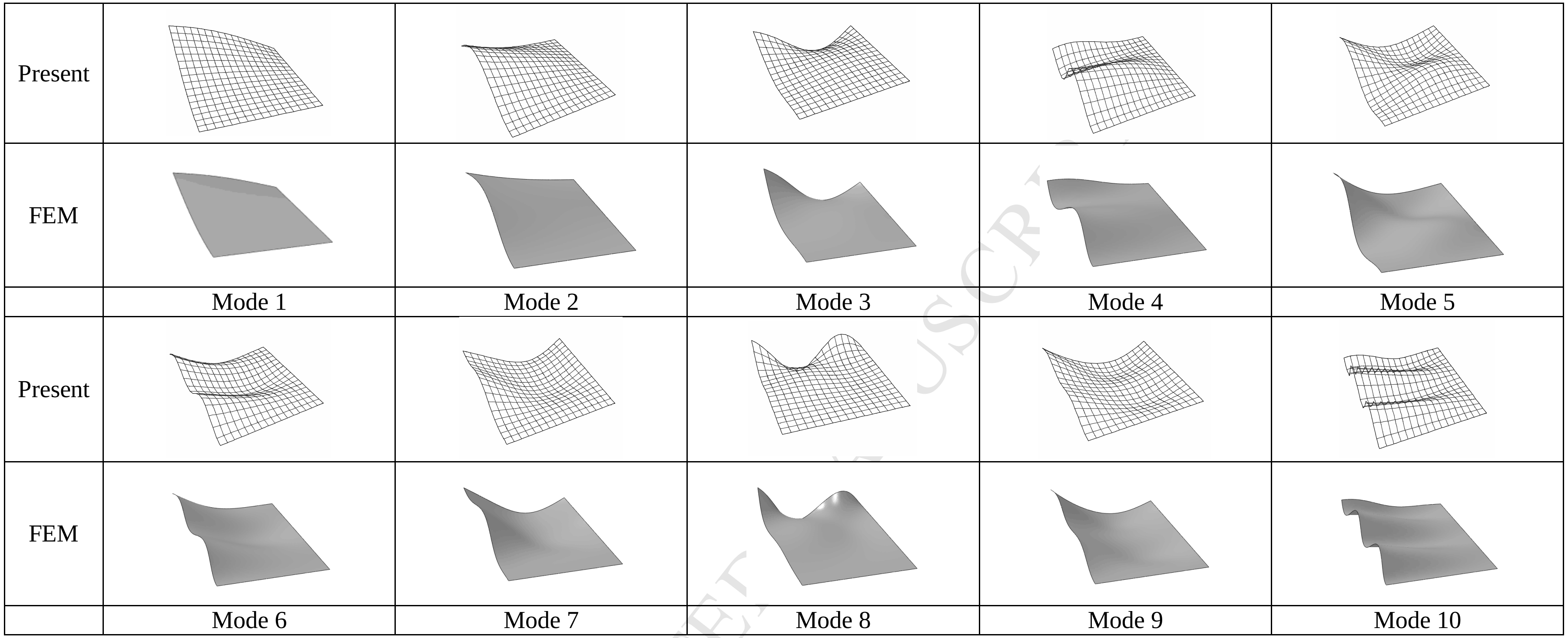

Fig. 5. First ten buckling modes of a uniaxially loaded CSFF square plate with $\kappa = 0$, $\gamma = 1$.

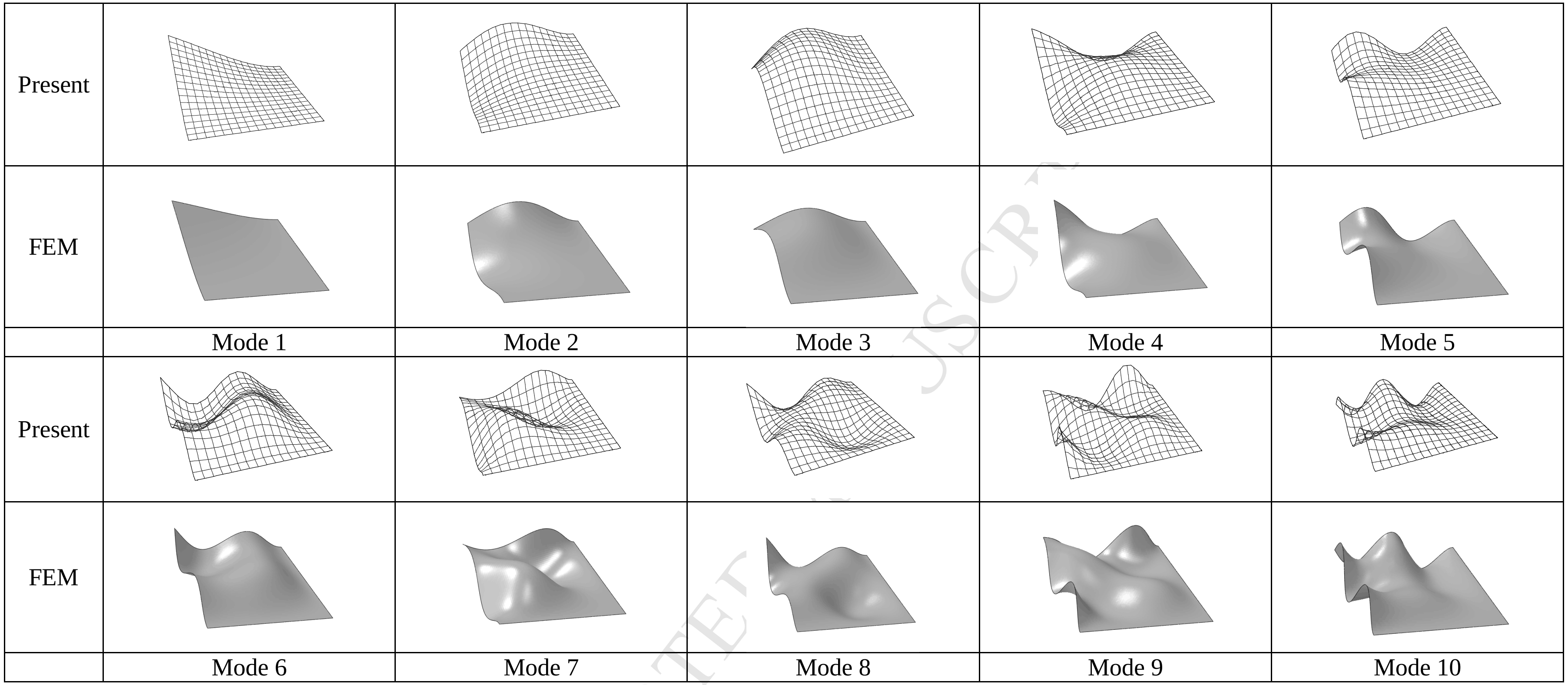

Fig. 6. First ten buckling modes of a biaxially loaded CCFF square plate with $\kappa = 1$, $\gamma = 1$.

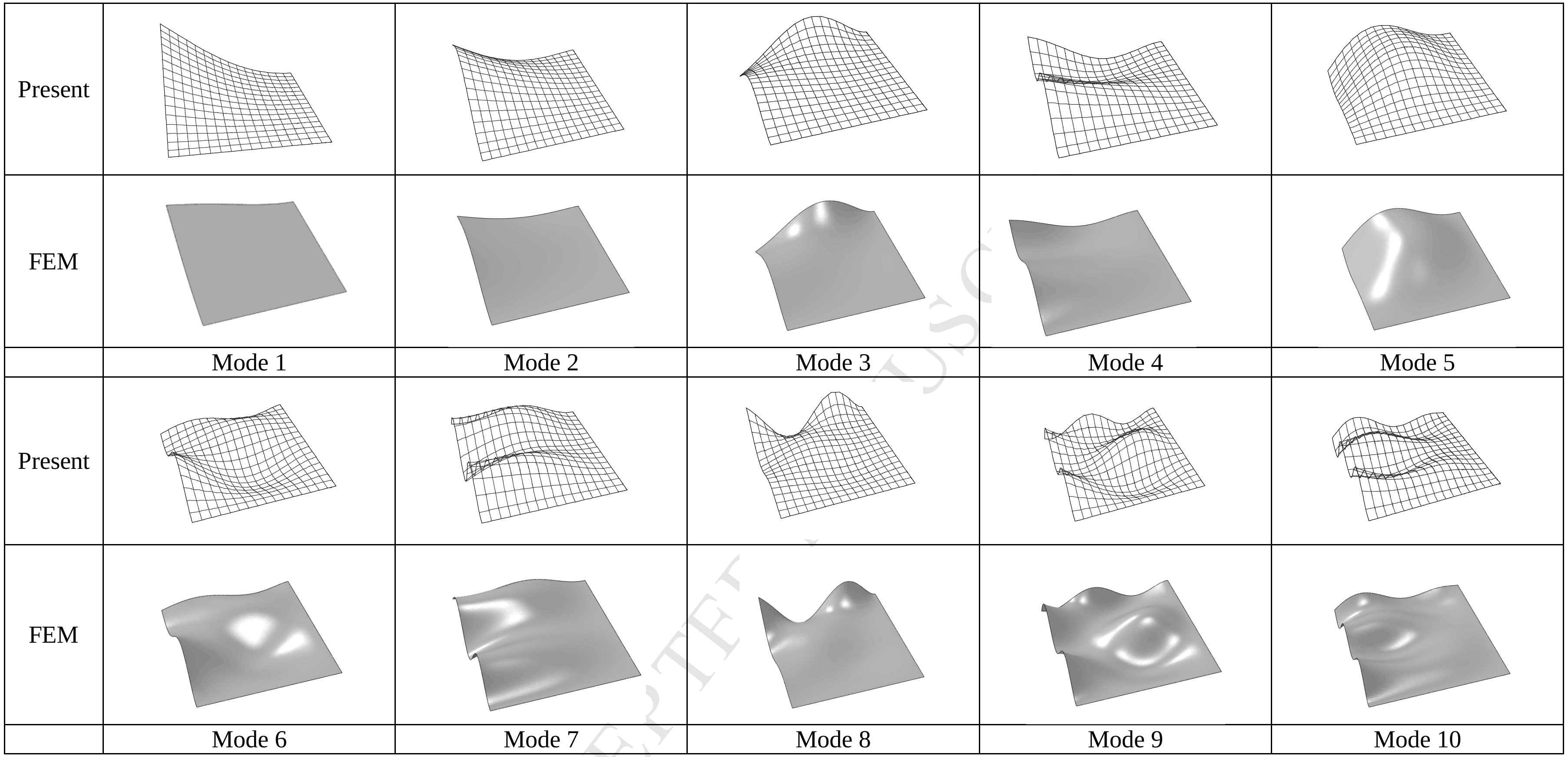

Fig. 7. First ten buckling modes of a biaxially loaded CCFF square plate with $\kappa = 1$, $\gamma = 5$.

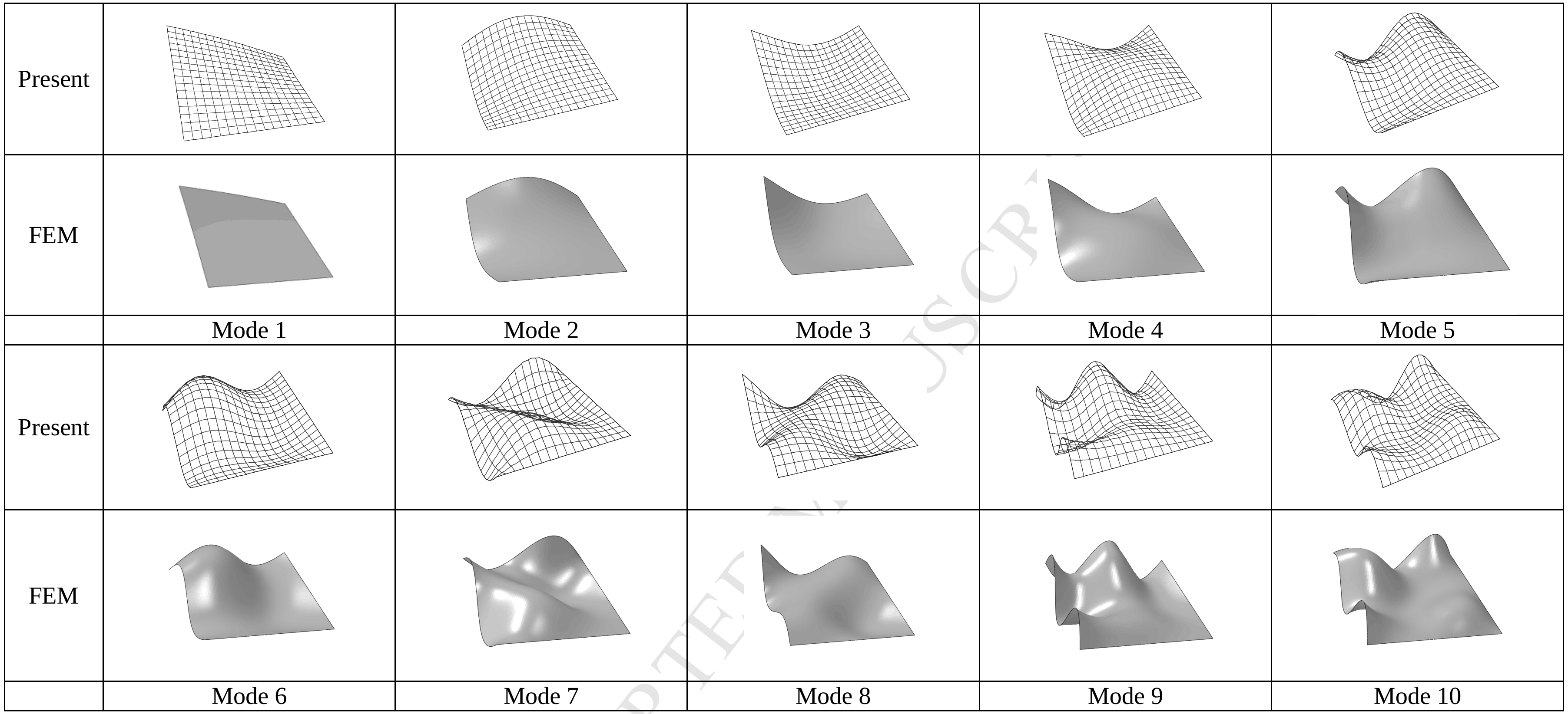

Fig. 8. First ten buckling modes of a biaxially loaded SSFF square plate with $\kappa = 1$, $\gamma = 1$.

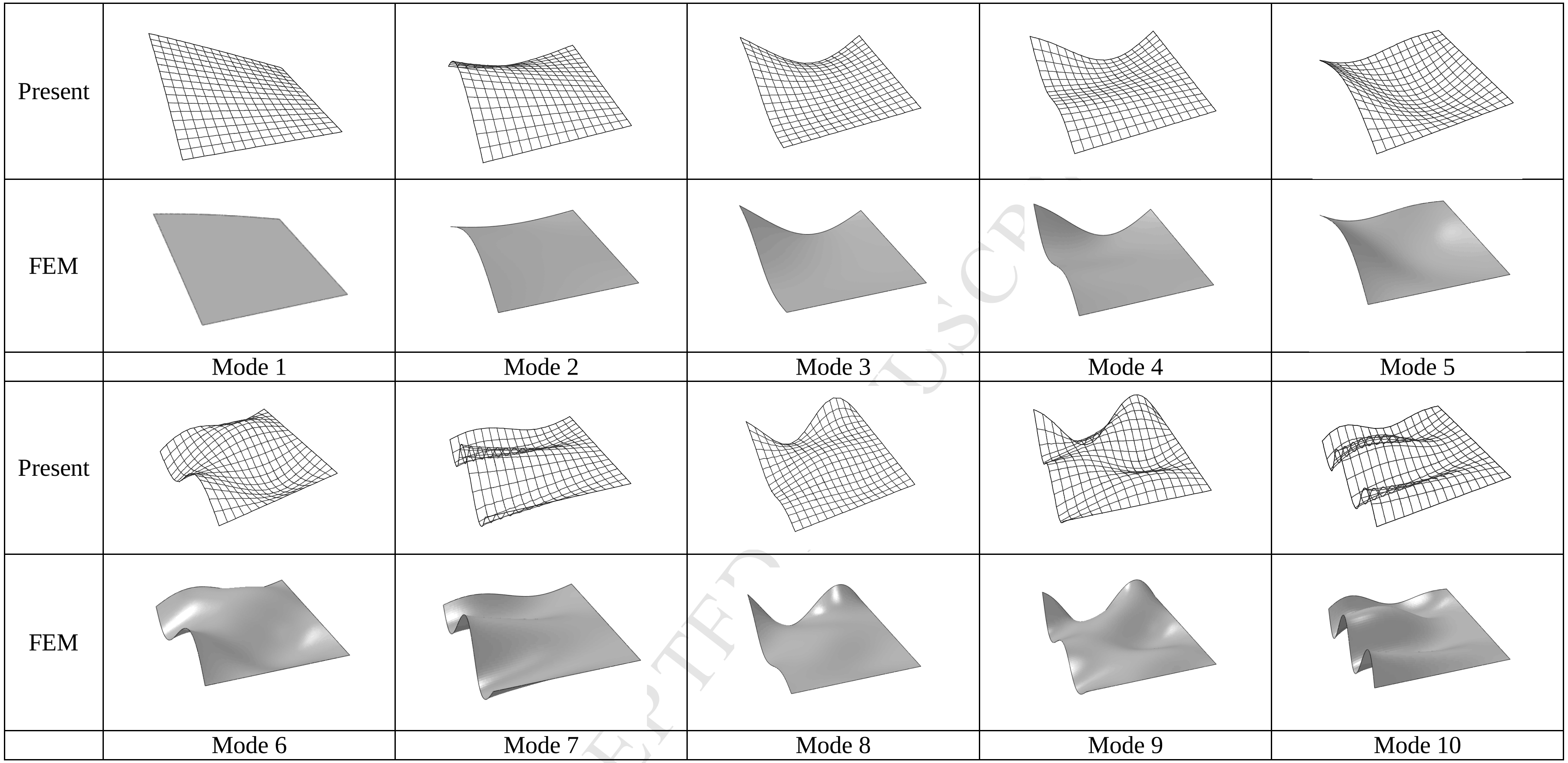

Fig. 9. First ten buckling modes of a biaxially loaded SSFF square plate with $\kappa = 1$, $\gamma = 5$.

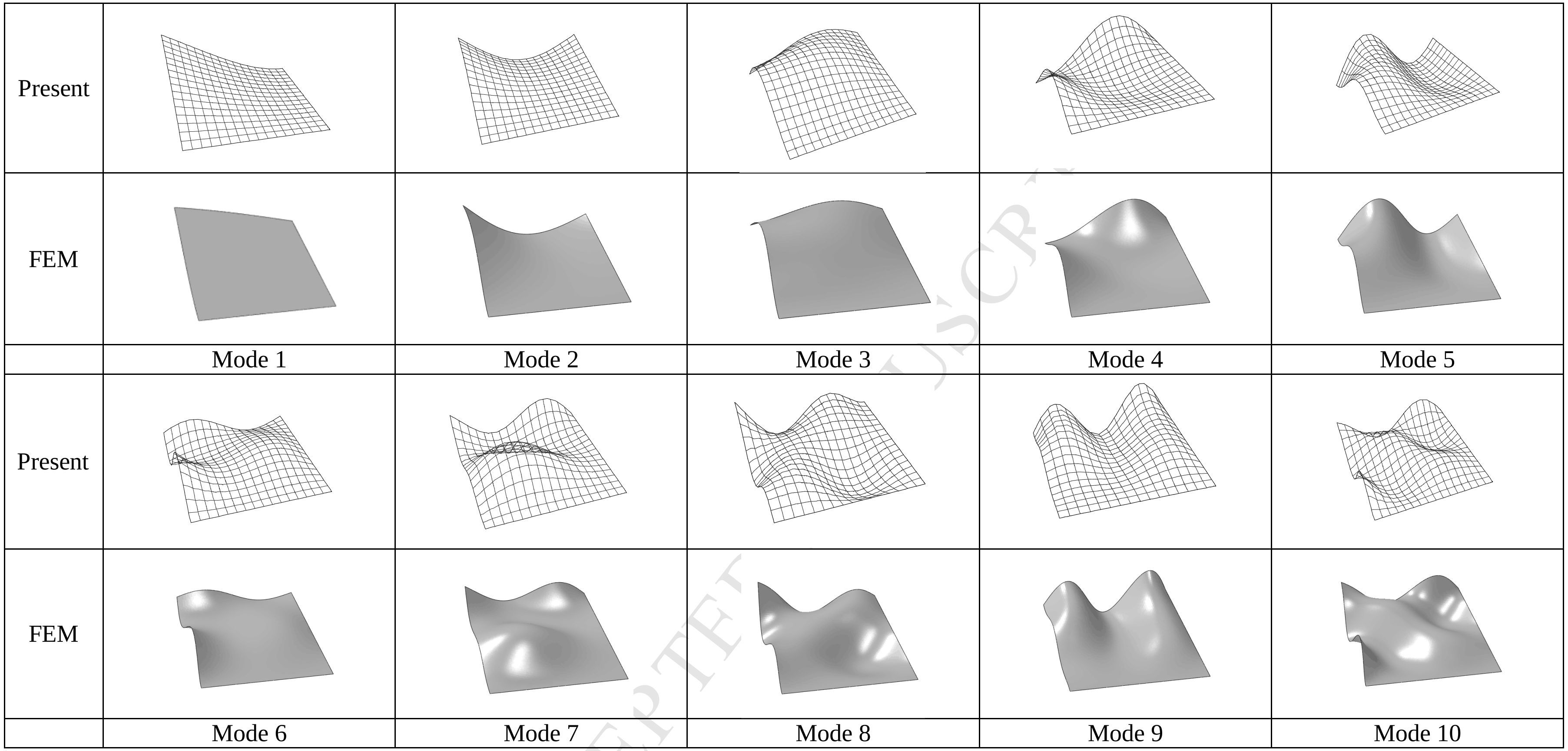

Fig. 10. First ten buckling modes of a biaxially loaded CSFF square plate with $\kappa = 1$, $\gamma = 1$.

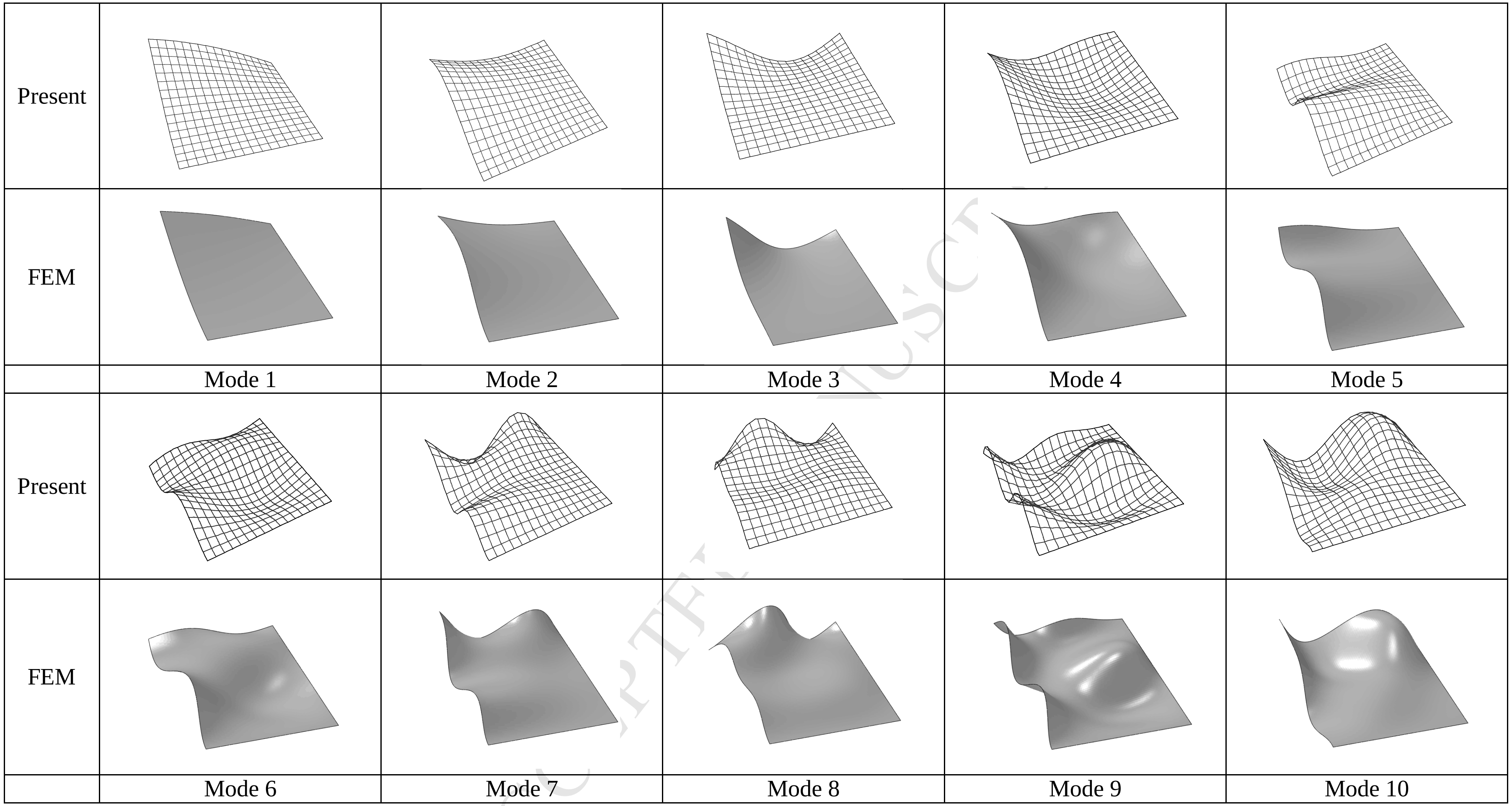

Fig. 11. First ten buckling modes of a biaxially loaded CSFF square plate with $\kappa = 1$, $\gamma = 5$.

Research Highlights

> Buckling of rectangular plates with two free adjacent edges is analytically solved.

> Novel symplectic superposition method is further developed for plate buckling.

> Distinctive merit of rigorous derivation helps to access new analytic solutions.